Advanced Review

Geometry optimization

H. Bernhard Schlegel*

Geometry optimization is an important part of most quantum chemical calculations. This article surveys methods for optimizing equilibrium geometries, locating transition structures, and following reaction paths. The emphasis is on optimizations using quasi-Newton methods that rely on energy gradients, and the discussion includes Hessian updating, line searches, trust radius, and rational function optimization techniques. Single-ended and double-ended methods are discussed for transition state searches. Single-ended techniques include quasi-Newton, reduced gradient following and eigenvector following methods. Double-ended methods include nudged elastic band, string, and growing string methods. The discussions conclude with methods for validating transition states and following steepest descent reaction paths. © 2011 John Wiley & Sons, Ltd. *WIREs Comput Mol Sci* 2011 1 790–809 DOI: 10.1002/wcms.34

INTRODUCTION

Geometry optimization is a key component of most computational chemistry studies that are concerned with the structure and/or reactivity of molecules. This chapter describes some of the methods that are used to optimize equilibrium geometries, locate transition structures (TSs), and follow reaction paths. Several surveys and reviews of geometry optimization are available.[1–14] Rather than an extensive review of the literature, this article is directed toward practical geometry optimization methods that are currently in use. In particular, it is concerned with geometry optimization methods applicable to electronic structure calculations.[15,16] Because electronic structure calculations can be lengthy, geometry optimization methods need to be efficient and robust. For inexpensive molecular mechanics calculations, simpler methods may be adequate. Most major electronic structure packages have a selection of geometry optimization algorithms. By discussing the components of various optimization methods we hope to aid the reader in selecting the most appropriate optimization methods and in overcoming the occasional difficulties that may arise. Unconstrained nonlinear optimization methods have been discussed extensively in numerical analysis texts (e.g., Refs 17–20). These methods are designed to find a local minimum closest to the starting point. Global optimization and conformational searching are more difficult problems and will be reviewed elsewhere in this series. Global mapping of reaction networks[21,22] is outside the scope of this chapter. Transition path sampling and reaction paths on free energy surfaces are also not covered.[23] Discussions of optimization methods to find conical intersections and minimum energy seam crossings can be found elsewhere.[22,24–36] Here, we focus on finding the equilibrium geometry of an individual molecule, locating a TS for a reaction, and following the reaction path connecting reactants through a TS to products. The geometry optimization methods discussed in this chapter use energy derivatives and depend on factors such as the choice of coordinates, methods for calculating the step direction, Hessian updating methods, line search, and step size control strategies. Some of these methods have been compared recently[37] for modest set of test cases for optimizing equilibrium geometries[38] and TSs.[39]

*Correspondence to: hbs@chem.wayne.edu

Department of Chemistry, Wayne State University, Detroit, MI, USA

DOI: 10.1002/wcms.34

POTENTIAL ENERGY SURFACES

The structure of a molecule can be specified by giving the locations of the atoms in the molecule. For a given structure and electronic state, a molecule has a specific energy. A potential energy surface describes how the energy of the molecule in a particular state varies as a function of the structure of the molecule. A simple representation of a potential energy surface is shown in Figure 1, in which the energy (vertical coordinate) is a function of two geometric variables (the two horizontal coordinates).

The notion of molecular structure and potential energy surfaces are outcomes of the Born–Oppenheimer approximation, which allows us

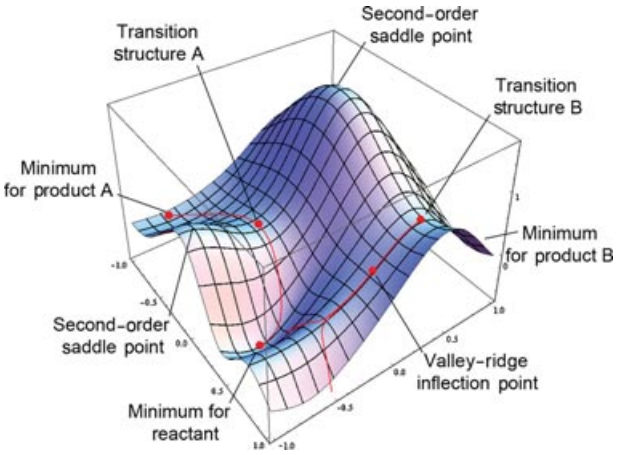

FIGURE 1 | Model potential energy surface showing minima, transition structures, second-order saddle points, reaction paths, and a valley ridge inflection point (Reprinted with permission from Ref 5. Copyright 1998 John Wiley & Sons.)

to separate the motion of the electrons from the motion of the nuclei. Because the nuclei are much heavier and move much more slowly than the electrons, the energy of a molecule in the Born–Oppenheimer approximation is obtained by solving the electronic structure problem for a set of fixed nuclear positions. Because this can be repeated for any set of nuclear positions, the energy of a molecule can be described as a parametric function of the position of the nuclei, thereby yielding a potential energy surface.

A potential energy surface, like the one shown in Figure 1, can be visualized as a hilly landscape, with valleys, peaks, and mountain passes. Even though most molecules have many more than two geometric variables, most of the important features of a potential energy surface can be represented in such a landscape.

The valleys of a potential energy surface represent reactants, intermediates, and products of a reaction. The position of the minimum in a valley represents the equilibrium structure. The energy difference between the product valley and reactant valley minima represents the energy of the reaction. Vibrational motion of the molecule about the reactant and product equilibrium geometries can be used to compute zero-point energy and thermal corrections needed to calculate enthalpy and free energy differences.[40] The lowest energy pathway between the reactant valley and the product valley is the reaction path.[41] The highest point on this lowest energy reaction path is the TS for the reaction, and the difference between the energy of the TS and the reactant is the energy barrier for the reaction. A TS is a maximum in one direction (the direction connecting reactant and product along the reaction path) and a minimum in all other directions (directions perpendicular to the reaction path). A TS is also termed as a first-order saddle point. In Figure 1, it can be visualized as a mountain pass connecting two valleys. A second-order saddle point (SOSP) is a maximum in two directions and a minimum in all the remaining directions. If a reaction path goes through an SOSP, a lower energy reaction path can always be found by displacing the path away from the SOSP. An *n*-th order saddle point is a maximum in *n* directions and a minimum in all the other directions.

For a thermally activated reaction, the energy of the TS and the shape of the potential energy surface around the TS can be used to estimate the reaction rate (see other reviews in this series). The steepest descent reaction path (SDP) from the TS down to the reactants and to the products is termed the minimum energy path (MEP) or the intrinsic reaction coordinate (IRC; the MEP in mass-weighted coordinates). The reaction path from reactants through intermediates (if any) to products describes the reaction mechanism.[41] A more detailed description of a reaction can be obtained by classical trajectory calculations[42–45] that simulate molecular dynamics by integrating the classical equations of motion for a molecule moving on a potential energy surface. Photochemistry involves motion on multiple potential energy surfaces and transitions between them (see Ref 46).

ENERGY DERIVATIVES

The first and second derivatives of the energy with respect to the geometrical parameters can be used to construct a local quadratic approximation to the potential energy surface:

$$E(\mathbf{x}) = E(\mathbf{x}_0) + \mathbf{g}_0^T \Delta\mathbf{x} + 1/2 \Delta\mathbf{x}^T \mathbf{H}_0 \Delta\mathbf{x} \qquad (1)$$

where $\mathbf{g}_0$ is the gradient ($dE/d\mathbf{x}$) at $\mathbf{x}_0$, $\mathbf{H}_0$ is the Hessian ($d^2E/d\mathbf{x}^2$) at $\mathbf{x}_0$, and $\Delta\mathbf{x} = \mathbf{x} - \mathbf{x}_0$. The gradient and Hessian can be used to confirm the character of minima and TSs. The negative of the gradient is the vector of forces on the atoms in the molecule. Because the forces are zero for minima, TSs, and higher-order saddle points, these structures are also termed stationary points. The Hessian or matrix of second derivatives of the energy is also known as the force constant matrix. The eigenvectors of the mass-weighted Hessian in Cartesian coordinates correspond to the normal modes of vibration (plus five or six modes for translation and rotation).[47] For a structure to be characterized as a minimum, the gradient

© 2011 John Wiley & Sons, Ltd.

17590884, 2011, 5, Downloaded from https://wires.onlinelibrary.wiley.com/doi/10.1002/wcms.34 by Research Institute for Healthcare Organization and Medical Management of Moscow Healthcare Department, Wiley Online Library on [12/05/2023]. See the Terms and Conditions (https://onlinelibrary.wiley.com/terms-and-conditions) on Wiley Online Library for rules of use; OA articles are governed by the applicable Creative Commons License

must be zero and all of the eigenvalues of the Hessian corresponding to molecular vibrations must be positive; equivalently, the vibrational frequencies must be real (the vibrational frequencies are proportional to the square root of the eigenvalues of the mass-weighted Hessian). For a TS, the potential energy surface is a maximum in one direction (along the reaction path) and a minimum in all other perpendicular directions. Therefore, a TS is characterized by a zero gradient and a Hessian that has one (and only one) negative eigenvalue; correspondingly, a TS has one and only one imaginary vibrational frequency. An n-th order saddle point (also called a stationary point of index n) has a zero gradient and is a maximum in n orthogonal directions and hence has n imaginary frequencies. For a TS, the vibrational mode corresponding to the imaginary frequency is also known as the transition vector. At the TS, the transition vector is tangent to the reaction path in mass-weighted coordinates.

Most methods for efficient geometry optimization rely on first derivatives of the energy; some also require second derivatives. For most levels of theory used routinely for geometry optimization, the first derivatives can be calculated analytically at a cost comparable to that for the energy. Analytic second derivatives are also available for several levels of theory, but the cost is usually considerably higher than for first derivatives. With the possible exception of optimization of diatomic molecules, derivative-based geometry optimization methods are significantly more efficient than energy-only algorithms. If analytic first derivatives are not available, it is possible to use simplex and pattern search methods,[48–50] but these become less efficient as the number of degree of freedom increases.[51] Thus, it may be more efficient to compute gradients numerically and to use a gradient-based optimization algorithm than to use an energy-only algorithm.

COORDINATES

In principle, any complete set of coordinates can be used to represent a molecule and its potential energy surface. However, choosing a good coordinate system can significantly improve the performance of geometry optimizations. Inspection of the Hessian used in the local quadratic approximation to the potential energy surface, in Eq. (1), can reveal some favorable aspects of a good coordinate system. For example, an optimization will be less efficient if there are some very stiff coordinates and some very flexible coordinates. This corresponds to a mixture of very large and very small eigenvalues of the Hessian, (i.e., the Hessian is an ill-conditioned matrix). Strong coupling between coordinates can also slow down an optimization. This corresponds to off-diagonal Hessian matrix elements that are comparable in magnitude to the diagonal elements. Strong anharmonicity can seriously degrade the performance of an optimization. If the Hessian changes rapidly when the geometry of the molecule is changed, or if the valley around a minimum is strongly curved, then the quadratic expression in Eq. (1) is a poor approximation to the potential energy surface and the optimization will be slow to converge. The nature of the Hessian and the anharmonicity of the potential energy surface will be directly affected by the choice of the coordinate system.

There are a number of coordinate systems that are typically used for geometry optimization. Cartesian coordinates are perhaps the most universal and the least ambiguous. An advantage is that most energy and derivative calculations are carried out in Cartesian coordinates. However, they are not well suited for geometry optimization because they do not reflect the 'chemical structure' and bonding of a molecule. The x, y, and z coordinates of an atom are strongly coupled to each other and to the coordinates of neighboring atoms.

Internal coordinates such as bond lengths and valence angles are more descriptive of the molecular structure and are more useful for geometry optimization. Bond stretching requires more energy than angle bending or torsion about single bonds. More importantly, the coupling between stretches, bends, and torsions are usually much smaller than between Cartesian coordinates. In addition, internal coordinates are much better than Cartesians for representing curvilinear motions such as valence angle bending and rotation about single bonds. For an acyclic molecule with N atoms, it is easy to select set of $3N-6$ internal coordinates to represent the molecule ($3N-5$ coordinates for a linear molecule). Z-matrix coordinates are an example of such a coordinate system.[52] It is straightforward to convert geometries and derivatives between Cartesian and Z-matrix internal coordinates.[53]

For acyclic molecules, the set of all bonds, angles, and torsions represents the intrinsic connectivity and flexibility of the molecule. However, for a cyclic molecule, this introduces more than the $3N-6$ coordinates required to define the geometry of the molecule. Such a coordinate system has a certain amount of redundancy in the geometric parameters.[53–68] Because only $3N-6$ of these redundant internal coordinates can be transformed back to Cartesian coordinates in three dimensions, certain combinations of the redundant internals must

 © 2011 John Wiley & Sons, Ltd.

17590884, 2011, 5, Downloaded from https://wires.onlinelibrary.wiley.com/doi/10.1002/wcms.34 by Research Institute for Healthcare Organization and Medical Management of Moscow Healthcare Department, Wiley Online Library on [12/05/2023]. See the Terms and Conditions (https://onlinelibrary.wiley.com/terms-and-conditions) on Wiley Online Library for rules of use; OA articles are governed by the applicable Creative Commons License

be constrained during the optimization. The set of all bonds, valence angles, and torsions (if necessary, augmented by out-of-plane bends and linear bends) constitutes a primitive redundant coordinate system.[53,58] In some cases, it may be advantageous to form linear combinations of the primitive redundant internals to form natural or delocalized redundant internal coordinates[54–57] or symmetry-adapted redundant internal coordinates. For periodic systems such as solids or surfaces, unit cell parameters need to be added[66–68] (either explicitly or implicitly via coordinates that cross the boundaries of the unit cell). For molecules in nonisotropic media, additional coordinates are needed to specify the orientation of the molecule. For systems containing more than one fragment, additional coordinates are required to specify the positions of the fragments relative to each other. The union of the redundant internal coordinates for the reactants and products is usually a good coordinate system for TS optimization.[58] The transformation of Cartesian coordinates and derivatives to redundant internals is straightforward, but the back transformation of a finite displacement of redundant internals to Cartesian usually is solved iteratively.[53–68]

NEWTON AND QUASI-NEWTON METHODS

As described in standard texts on optimization,[17–20] most nonlinear optimization algorithms are based on a local quadratic approximation of the potential energy surface; Eq. (1). Differentiation with respect to the coordinates yields an approximation for the gradient, given by:

$$\mathbf{g}(\mathbf{x}) = \mathbf{g}_0 + \mathbf{H}_0 \Delta\mathbf{x}. \tag{2}$$

At a stationary point, the gradient is zero, $\mathbf{g}(\mathbf{x}) = \mathbf{0}$; thus, in the local quadratic approximation to the potential energy surface, the displacement to the minimum is given by:

$$\Delta\mathbf{x} = -\mathbf{H}_0^{-1}\mathbf{g}_0. \tag{3}$$

This is known as the Newton or Newton–Raphson step.

Newton and quasi-Newton methods are the most efficient and widely used procedures for optimizing equilibrium geometries and can also be used effectively to find TSs. For each step in the Newton method, the Hessian in Eq. (3) is calculated at the current point. For quasi-Newton methods, Eq. (3) is used with an approximate Hessian that is updated at each step of the optimization (see below). Because actual potential energy surfaces are rarely quadratic, several Newton or quasi-Newton steps are required to reach a stationary point. For minimization, the Hessian must have all positive eigenvalues (i.e., positive definite). If one or more eigenvalues are negative, the step will be toward a first or higher-order saddle point. Thus, without some means of controlling the step size and direction, simple Newton steps are not robust. Similarly, if the aim is to optimize to a TS, the Hessian must have one and only one negative eigenvalue, and the corresponding eigenvector (i.e., the transition vector) must be roughly parallel to the reaction path. Methods for ensuring that the step is in the desired direction for minimization or TS optimization are discussed in the section dealing with step size control.

At each step, Newton methods require the explicit calculation of the Hessian, which can be rather costly. Quasi-Newton methods start with an inexpensive approximation to the Hessian. The difference between the calculated change in the gradient and the change predicted with the approximate Hessian is used to improve the Hessian at each step in the optimization.[17–20]

$$\mathbf{H}^{\text{new}} = \mathbf{H}^{\text{old}} + \Delta\mathbf{H} \tag{4}$$

For a quadratic surface, the updated Hessian must fulfill the Newton condition,

$$\Delta\mathbf{g} = \mathbf{H}^{\text{new}}\Delta\mathbf{x}, \tag{5}$$

where $\Delta\mathbf{g} = \mathbf{g}(\mathbf{x}^{\text{new}}) - \mathbf{g}(\mathbf{x}^{\text{old}})$ and $\Delta\mathbf{x} = (\mathbf{x}^{\text{new}} - \mathbf{x}^{\text{old}})$. However, there are an infinite number of ways to update the Hessian and fulfill the Newton condition. One of the simplest updates is the symmetric rank one (SR1) update,[17–20] also known as the Murtagh–Sargent update.[69]

$$\Delta\mathbf{H}^{\text{SR1}} = \frac{(\Delta\mathbf{g} - \mathbf{H}^{\text{old}}\Delta\mathbf{x})\,(\Delta\mathbf{g} - \mathbf{H}^{\text{old}}\Delta\mathbf{x})^T}{(\Delta\mathbf{g} - \mathbf{H}^{\text{old}}\Delta\mathbf{x})^T\Delta\mathbf{x}} \tag{6}$$

This formula can encounter numerical problems if $|\Delta\mathbf{g} - \mathbf{H}^{\text{old}}\Delta\mathbf{x}|$ is very small. The Broyden family of updates[70] avoids this problem while ensuring that the Hessian update is positive definite. The Broyden–Fletcher–Goldfarb–Shanno (BFGS) update[70–73] is the most successful and widely used member of this family:

$$\Delta\mathbf{H}^{\text{BFGS}} = \frac{\Delta\mathbf{g}\,\Delta\mathbf{g}^T}{\Delta\mathbf{g}^T\Delta\mathbf{x}} - \frac{\mathbf{H}^{\text{old}}\Delta\mathbf{x}\,\Delta\mathbf{x}^T\mathbf{H}^{\text{old}}}{\Delta\mathbf{x}^T\mathbf{H}^{\text{old}}\Delta\mathbf{x}}. \tag{7}$$

For TS optimization, it is important that the Hessian has one and only one negative eigenvalue. This should be checked at every step of the optimization. If the Hessian does not have the correct number of negative eigenvalues, the eigenvalues need to be shifted or one of the methods for step size control

© 2011 John Wiley & Sons, Ltd.

17590884, 2011, 5, Downloaded from https://wires.onlinelibrary.wiley.com/doi/10.1002/wcms.34 by Research Institute for Healthcare Organization and Medical Management of Moscow Healthcare Department, Wiley Online Library on [12/05/2023]. See the Terms and Conditions (https://onlinelibrary.wiley.com/terms-and-conditions) on Wiley Online Library for rules of use; OA articles are governed by the applicable Creative Commons License

needs to be used (see *Step Size Control*). The initial estimate of the Hessian for TS optimizations must have one negative eigenvalue and the associated eigenvector should be approximately parallel to the reaction path. The Hessian update should not be forced to be positive definite. The Powell-symmetric-Broyden (PSB) update[18] fulfills this role:

$$\Delta\mathbf{H}^{\mathrm{PSB}} = \frac{(\Delta\mathbf{g} - \mathbf{H}^{\mathrm{old}}\Delta\mathbf{x})\Delta\mathbf{x}^T + \Delta\mathbf{x}\,(\Delta\mathbf{g} - \mathbf{H}^{\mathrm{old}}\Delta\mathbf{x})^T}{\Delta\mathbf{x}^T\Delta\mathbf{x}} - \frac{(\Delta\mathbf{x}^T(\Delta\mathbf{g} - \mathbf{H}^{\mathrm{old}}\Delta\mathbf{x}))\,\Delta\mathbf{x}\,\Delta\mathbf{x}^T}{(\Delta\mathbf{x}^T\Delta\mathbf{x})^2}. \quad (8)$$

Bofill[74] found that a combination of the PSB and SR1 updates performs better for TS optimizations:

$$\Delta\mathbf{H}^{\mathrm{Bofill}} = \phi\Delta\mathbf{H}^{\mathrm{SR1}} + (1-\phi)\Delta\mathbf{H}^{\mathrm{PSB}},$$
$$\text{where} \quad \phi = \frac{((\Delta\mathbf{g} - \mathbf{H}^{\mathrm{old}}\Delta\mathbf{x})^T\Delta\mathbf{x})^2}{|\Delta\mathbf{g} - \mathbf{H}^{\mathrm{old}}\Delta\mathbf{x}|^2\,|\Delta\mathbf{x}|^2}. \quad (9)$$

Farkas and Schlegel[75] constructed a similar update for minimization:

$$\Delta\mathbf{H}^{\mathrm{FS}} = \phi^{1/2}\Delta\mathbf{H}^{\mathrm{SR1}} + (1-\phi^{1/2})\Delta\mathbf{H}^{\mathrm{BFGS}}, \quad (10)$$

where ϕ is same as in Eq. (9). Bofill[76] has recently reviewed Hessian updating methods and proposed some promising new formulas suitable for minima and TSs. For controlling the step size by trust radius (τ) methods or rational function optimization (see *Step Size Control*), diagonalizing the Hessian can become a computational bottleneck for large systems. Updating the eigenvectors and eigenvalues of the Hessian can be considerably more efficient.[77]

Quasi-Newton methods require an initial estimate of the Hessian. A scaled identity matrix may be sufficient in some cases, but a better starting Hessian can be obtained from knowledge of the structure and connectivity of the molecule. Simple empirical estimates of stretching, bending, and torsional force constants are usually satisfactory.[78–80] Calculation of an initial Hessian by molecular mechanics or semi-empirical electronic structure methods can provide a better estimate. If the molecule has been optimized at a lower level of theory, the updated Hessian from the optimization or the Hessian from a frequency calculation at a lower level of theory are even better initial estimates. For harder cases, the rows and columns of the Hessian can be calculated numerically for a few critical coordinates. For more difficult cases, the full Hessian can be calculated at the beginning of the optimization and recalculated at every few step if necessary. Recalculating the Hessian at each step corresponds to the Newton method.

Standard quasi-Newton methods store and invert the full Hessian. For large optimization problems, this may be a bottleneck. The updating methods can be reformulated to update the inverse of the Hessian. For example, the BFGS formula for the update of the inverse Hessian is:

$$\Delta\mathbf{B}^{\mathrm{BFGS}} = \frac{\Delta\mathbf{x}\Delta\mathbf{x}^T}{\Delta\mathbf{x}^T\Delta\mathbf{g}} - \frac{\mathbf{B}^{\mathrm{old}}\Delta\mathbf{g}\Delta\mathbf{g}^T\mathbf{B}^{\mathrm{old}}}{\Delta\mathbf{g}^T\mathbf{B}^{\mathrm{old}}\Delta\mathbf{g}}, \quad (11)$$

where $\mathbf{B} = \mathbf{H}^{-1}$, and the updated inverse Hessian obeys $\Delta\mathbf{x} = \mathbf{B}\Delta\mathbf{g}$. Limited memory quasi-Newton methods such as L-BFGS[80–89] avoid the storage of the full Hessian or its inverse which would require $O(n^2)$ memory for n variables. Instead, they start with a diagonal inverse Hessian, and store only the $\Delta\mathbf{x}$ and $\Delta\mathbf{g}$ vectors from a limited number of previous steps; thus, the storage is only $O(n)$. The inverse Hessian is written as a diagonal Hessian plus the updates using the stored vectors. For the Newton step, $\mathbf{x}^{\mathrm{new}} = \mathbf{x}^{\mathrm{old}} - \mathbf{B}\,\mathbf{g}^{\mathrm{old}}$, the product of the updated inverse Hessian and the gradient involves only $O(n)$ work because it can be expressed in terms of dot products between vectors.

CONJUGATE GRADIENT METHODS

Conjugate gradient methods are suitable for very large systems because they require less storage than limited memory quasi-Newton methods. The concept behind conjugate gradient methods is to choose a new search direction that will lower the energy while remaining at or near the minimum in the previous search direction. If the Hessian has coupling between the coordinates, the optimal search directions are not orthogonal but are conjugate, in the sense that $\Delta\mathbf{x}^{\mathrm{new}}\,\mathbf{H}\Delta\mathbf{x}^{\mathrm{old}} = 0$. Two of the most frequently used conjugate gradient methods are Fletcher–Reeves[90] and Polak-Ribiere[91]:

$$\mathbf{s}_i = -\mathbf{g}_i + \frac{\mathbf{g}_i^T\mathbf{g}_i}{\mathbf{g}_{i-1}^T\mathbf{g}_{i-1}}\,\mathbf{s}_{i-1} \quad (12)$$

$$\mathbf{s}_i = -\mathbf{g}_i + \frac{(\mathbf{g}_i - \mathbf{g}_{i-1})^T\mathbf{g}_i}{\mathbf{g}_{i-1}^T\mathbf{g}_{i-1}}\,\mathbf{s}_{i-1}, \quad (13)$$

where $\mathbf{s}_i$ and $\mathbf{s}_{i-1}$ are the current and previous search directions, respectively, and $\mathbf{g}_i$ and $\mathbf{g}_{i-1}$ are the current and previous gradients, respectively. Note that only three vectors need to be stored. Unlike quasi-Newton methods, conjugate gradient methods require a line search at each step in order to converge.

GDIIS

Direct inversion of the iterative subspace (DIIS) constructs a solution to a set of linear equations such as Eq. (3) by expanding in a set of error vectors or

© 2011 John Wiley & Sons, Ltd.

17590884, 2011, 5, Downloaded from https://wires.onlinelibrary.wiley.com/doi/10.1002/wcms.34 by Research Institute for Healthcare Organization and Medical Management of Moscow Healthcare Department, Wiley Online Library on [12/05/2023]. See the Terms and Conditions (https://onlinelibrary.wiley.com/terms-and-conditions) on Wiley Online Library for rules of use; OA articles are governed by the applicable Creative Commons License

residuals from prior iterations. Geometry optimization by DIIS (GDIIS) applies this approach to the optimization of equilibrium geometries and transition structures.[92–95] In the numerical analysis literature, DIIS is known as generalized minimum of the residual (GMRES).[96] It has its origins in methods like the Krylov,[97] Lanczos,[98] and Arnoldi[99] algorithms. In GDIIS, the goal is to construct a new geometry as a linear combination of previous geometries so as to minimize the size of the Newton step [i.e., the residual in the iterative solution of Eq. (3)].

$$\mathbf{x}^* = \sum_i c_i\,\mathbf{x}_i \quad \mathbf{g}^* = \sum_i c_i\,\mathbf{g}(\mathbf{x}_i) \quad \sum_i c_i = 1 \tag{14}$$

$$\text{Minimize } |\mathbf{x}^{\text{new}} - \mathbf{x}^*|^2 \text{ with respect to } c_i,$$
$$\text{where } \mathbf{x}^{\text{new}} = \mathbf{x}^* - \mathbf{H}^{-1}\mathbf{g}^* \tag{15}$$

The GDIIS coefficients are determined by minimizing the residual and can be obtained by solving the following:

$$\begin{bmatrix}\mathbf{A} & \mathbf{1}\\ \mathbf{1} & 0\end{bmatrix}\begin{bmatrix}\mathbf{c}\\ \lambda\end{bmatrix} = \begin{bmatrix}\mathbf{0}\\ 1\end{bmatrix},$$
$$\text{where} \quad A_{ij} = (\mathbf{H}^{-1}\mathbf{g}_i)^T(\mathbf{H}^{-1}\mathbf{g}_j). \tag{16}$$

The GEDIIS method[95] uses $\mathbf{A}_{ij} = (\mathbf{g}_i - \mathbf{g}_j)\,(\mathbf{x}_i - \mathbf{x}_j)$. If $\mathbf{A}$ becomes singular, the oldest geometry is discarded and the solution is attempted again. The approximate Hessian can be held constant, but better performance is obtained if it is updated. If the minimization wanders into a region with a negative eigenvalue, it may converge to a TS. For a TS optimization, GDIIS sometimes converges not to the desired reaction barrier but to the nearest saddle point. One way to control GDIIS optimizations is to compare the predicted geometry with the one from a Newton step.[94] If the angle is too large, it is safer to take the Newton step (provided the Hessian has the correct number of negative eigenvalues). In the final stages of a minimization, GDIIS sometimes converges faster than quasi-Newton methods; a hybrid of quasi-Newton and DIIS methods can be more efficient.[95]

LINE SEARCH

Newton, quasi-Newton, and GDIIS methods will converge without a line search if the surface is quadratic. However, life is not quadratic. For anharmonic surfaces, the Newton step (Eq. (3)) may be too large or too small. Near an inflection point, Newton steps can get into an infinite hysteresis loop. Conjugate gradient methods need a line search because they generate only a search direction but not a step length. Thus, a line search is a good idea for any method, especially if it can be done with little or no extra cost. The line search need not be exact but must fulfill the Wolfe condition, $\Delta E < \alpha\,\mathbf{g}^T\Delta\mathbf{x}$ and $\mathbf{g}^{\text{new}\,T}\Delta\mathbf{x} > \beta\,\mathbf{g}^{\text{old}\,T}\Delta\mathbf{x}$, reducing the function value and the magnitude of the gradient ($\alpha \approx 0.1$ and $\beta \approx 0.5$ have been found to be practical for quasi-Newton optimizations[18]). A simple approach is to fit a polynomial to the energy and gradient at the current and the previous geometry (a cubic polynomial or a quartic polynomial constrained to have no negative second derivatives[100]). The minimum is found on the polynomial, the gradient is interpolated to the minimum, and the interpolated gradient is used for the next quasi-Newton step. If there is a large extrapolation to the minimum, it is safer to explicitly search for the minimum by doing additional energy (and gradient) calculations to obtain a sufficient reduction in the energy (and the magnitude of the gradient).

STEP SIZE CONTROL

The quadratic approximation to the potential energy surface is satisfactory only for a small local region, usually specified by a trust radius, τ. Steps outside this region are risky and optimizations are more robust if the step size does not exceed τ. An initial estimate of τ can be updated during the course of an optimization based on how well the potential energy surface can be fit by a quadratic expression. A typical updating recipe is as follows[18]:

$$\rho = \Delta E/(\mathbf{g}^T\Delta\mathbf{x} + 1/2\,\Delta\mathbf{x}^T\,\mathbf{H}_0\,\Delta\mathbf{x}).$$
$$\text{If } \rho > 0.75 \text{ and } 5/4\,|\Delta\mathbf{x}| > \tau^{\text{old}},$$
$$\text{then } \tau^{\text{new}} = 2\,\tau^{\text{old}}.$$
$$\text{If } \rho < 0.25, \text{ then } \tau^{\text{new}} = 1/4\,|\Delta\mathbf{x}|.$$
$$\text{Otherwise, } \tau^{\text{new}} = \tau^{\text{old}}. \tag{17}$$

The simplest approach to step size control is to scale the Newton step back if τ is exceeded. A better approach is to minimize the energy under the constraint that the step is not larger than τ.[18,20] In the trust radius method (TRM), this is done by using a Lagrangian multiplier, λ, and corresponds to minimizing $E(\mathbf{x}) - 1/2\ \lambda\ (\Delta\mathbf{x}^2 - \tau^2)$. With the usual quadratic approximation for $E(\mathbf{x})$, this yields:

$$\mathbf{g}_0 + \mathbf{H}_0\Delta\mathbf{x} - \lambda\Delta\mathbf{x} = 0$$
$$\text{or} \quad \Delta\mathbf{x} = -(\mathbf{H}_0 - \lambda\mathbf{I})^{-1}\mathbf{g}_0 \tag{18}$$

where $\mathbf{I}$ is the identity matrix.

For minimizations, λ must be chosen so that all the eigenvalues of the shifted Hessian, $\mathbf{H} - \lambda\,\mathbf{I}$, are positive [i.e., λ must be smaller (more negative) than the lowest eigenvalue of $\mathbf{H}$]. Thus, even if $\mathbf{H}$ has one or

© 2011 John Wiley & Sons, Ltd.

17590884, 2011, 5, Downloaded from https://wires.onlinelibrary.wiley.com/doi/10.1002/wcms.34 by Research Institute for Healthcare Organization and Medical Management of Moscow Healthcare Department, Wiley Online Library on [12/05/2023]. See the Terms and Conditions (https://onlinelibrary.wiley.com/terms-and-conditions) on Wiley Online Library for rules of use; OA articles are governed by the applicable Creative Commons License

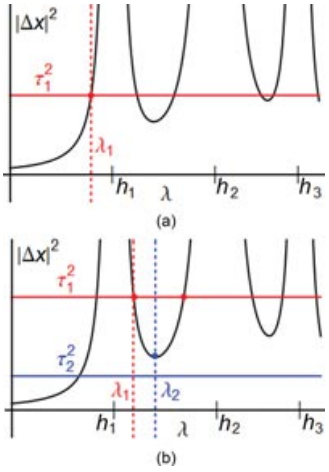

FIGURE 2 | Plot of the displacement squared, $|\Delta x|^2 = |(H - \lambda I)^{-1} g|^2$, as a function of the Hessian shift parameter λ (Reprinted with permission from Ref 102. Copyright 1983 ACS Publications.). The singularties occur at the eigenvalues of the Hessian, h_i. (a) For displacement to a minimum with a trust radius of τ_1, shift parameter λ_1 must be less than the lowest eigenvalue of the Hessian, h_1. (b) For a displacement to a transition structure, the shift parameter must be between h_1 and $\frac{1}{2}\ h_2$. For τ_1, the lower of the two solutions is chosen. For a smaller trust radius τ_2, there is no solution; λ_2 is chosen as the minimum in the curve [or $\lambda_2 = \frac{1}{2}\ (h_1 + \frac{1}{2}\ h_2)$ if $\lambda_2 > \frac{1}{2}\ h_2$] and the displacement is scaled back to the trust radius (see Refs 101–104 for more details).

more negative eigenvalues, this approach can be used to take a controlled step downhill toward a minimum. A plot of the square of step size as a function of λ is shown in Figure 2(a) (the singularities occur when λ is equal to one of the eigenvalues of **H**).

For TS optimization, the shifted Hessian must have one negative eigenvalue (i.e., λ must be larger than the lowest eigenvalue of **H** but smaller than the second lowest eigenvalue). As shown in Figure 2(b), if there are two solutions for a given step size, λ is usually chosen to be closer to the lowest eigenvalue; if there are no solutions for a given step size, λ is chosen as the minimum between the lowest and second lowest eigenvalue and the resulting step is scaled back to the τ.[101–104] This procedure then allows a controlled step to be taken toward the TS even when the Hessian does not have the correct number of negative eigenvalues.

An alternative approach for TS optimization is to use the eigenvectors of the approximate Hessian to divide the coordinates into two groups; the optimization then searches for a maximum along one eigenvector and for a minimum in the remaining space. The step size in this approach can be controlled by using two Lagrangian multipliers, one for the step uphill along one eigenvector and the other for the step downhill in the remainder of the space. Because this approach allows one to follow an eigenvector uphill even if it does not have the lowest eigenvalue, it is also known as eigenvector following.[74,101–109] Alternatively, a separate λ can be chosen for each eigenvector such that the step varies from steepest descent for large gradients to a Newton step with a shifted Hessian for moderate gradients to a simple Newton step for small gradients.[2] For all of these approaches to transition structure optimization, the Hessian must have a suitable eigenvector that resembles the desired reaction path. Instead of focusing on a single eigenvector, the reduced potential surface approach selects a small subset of the coordinates for the transition structure search and minimizes the energy in the remaining space.[110,111]

The rational function optimization (RFO) method is a closely related approach for controlling the step size for both minimization and transition structure searching that replaces the quadratic approximation by a rational function approximation.[105]

$$\Delta E(\mathbf{x}) = \frac{\mathbf{g}^T \Delta\mathbf{x} + 1/2 \Delta\mathbf{x}^T \mathbf{H} \Delta\mathbf{x}}{1 + \Delta\mathbf{x}^T \mathbf{S} \Delta\mathbf{x}} = \frac{1}{2} \frac{[\Delta\mathbf{x} \quad 1] \begin{bmatrix} \mathbf{H} & \mathbf{g} \\ \mathbf{g}^T & 0 \end{bmatrix} \begin{bmatrix} \Delta\mathbf{x} \\ 1 \end{bmatrix}}{[\Delta\mathbf{x} \quad 1] \begin{bmatrix} \mathbf{S} & 0 \\ 0 & 1 \end{bmatrix} \begin{bmatrix} \Delta\mathbf{x} \\ 1 \end{bmatrix}} \tag{19}$$

Minimizing ΔE with respect to $\Delta\mathbf{x}$ by setting $\mathrm{d}\Delta E/\mathrm{d}\Delta\mathbf{x} = \mathbf{0}$ leads to an eigenvalue equation involving the Hessian augmented by the gradient.

$$\begin{bmatrix} \mathbf{H} & \mathbf{g} \\ \mathbf{g}^T & 0 \end{bmatrix} \begin{bmatrix} \Delta\mathbf{x} \\ 1 \end{bmatrix} = 2\ \Delta E \begin{bmatrix} \mathbf{S} & 0 \\ 0 & 1 \end{bmatrix} \begin{bmatrix} \Delta\mathbf{x} \\ 1 \end{bmatrix} \tag{20}$$

Typically, **S** is chosen as a constant times the identity matrix [in this case the top row of Eq. (20) reduces to $\Delta\mathbf{x} = -(\mathbf{H}_0 - \lambda\mathbf{I})^{-1}\mathbf{g}_0$, as in TRM; Eq. (18)]. The lowest eigenvalue and eigenvector of the augmented Hessian are used for minimizations, whereas the second lowest eigenvalue and eigenvector are chosen for transition structure optimizations. The $\Delta\mathbf{x}$ obtained by the RFO approach is reduced if it is larger than the τ.[105,106,108,109] A partitioned RFO method may be better for saddle point searches if the Hessian does not have the correct number of negative eigenvalues.[105] In this case, one eigenvector is chosen to be followed uphill to a maximum and the remaining eigenvectors are chosen for minimization; the RFO method is used for optimization in both subspaces. It is possible to reach other transition structures by following an eigenvector other than the one with the lowest eigenvalue.[105–109]

© 2011 John Wiley & Sons, Ltd.

17590884, 2011, 5, Downloaded from https://wires.onlinelibrary.wiley.com/doi/10.1002/wcms.34 by Research Institute for Healthcare Organization and Medical Management of Moscow Healthcare Department, Wiley Online Library on [12/05/2023]. See the Terms and Conditions (https://onlinelibrary.wiley.com/terms-and-conditions) on Wiley Online Library for rules of use; OA articles are governed by the applicable Creative Commons License

CONSTRAINED OPTIMIZATION

Under a variety of circumstances, it may be necessary to apply constraints while optimizing the geometry (e.g., scanning potential energy surfaces, coordinate driving, reaction path following, etc.). For nonredundant coordinate systems and simple constraints, the coordinates being held constant can be easily removed from the space of variables being optimized. For more general constraints and/or redundant internal coordinate systems, constraints can be applied by penalty functions, projection methods, or Lagrangian multipliers.

In the penalty function method, the constraints $C_i(\mathbf{x}) = 0$ are imposed by adding an extra term, $1/2 \sum \alpha_i C_i(\mathbf{x})^2$, to the energy in Eq. (1) and the energy is minimized as usual. Because the α_i's need to have suitably large values so that the constraints are approximately satisfied at the minimum, the optimization may converge much slower than the corresponding unconstrained optimization.

The preferred method for including constraints in an optimization is by using Lagrangian multipliers.

$$L(\mathbf{x}) = E(\mathbf{x}) + \sum_i \lambda_i C_i(\mathbf{x}) \tag{21}$$

At convergence of the constrained optimization, the derivative of the Lagrangian $L(\mathbf{x})$ with respect to the coordinate $\mathbf{x}$ and the Lagrangian multiplier λ_i must be zero. In the LQA,

$$\frac{\partial L(\mathbf{x})}{\partial \mathbf{x}} = \mathbf{g}_0 + \mathbf{H}_0 \Delta\mathbf{x} + \sum_i \lambda_i \frac{\partial C_i(\mathbf{x})}{\partial \mathbf{x}} = 0$$

$$\text{and} \quad \frac{\partial L(\mathbf{x})}{\partial \lambda_i} = C_i(\mathbf{x}) = 0. \tag{22}$$

Because the Lagrangian multipliers are optimized along with the geometric variables, this method generally converges much faster than the penalty function method and the constraints are satisfied exactly. In the special case in which the constraint is linear function of the displacements, $\mathbf{c}^T\Delta\mathbf{x} = c_0$, the Lagrangian multiplier problem can be solved by using an augmented Hessian,

$$\mathbf{g}_0 + \mathbf{H}_0\Delta\mathbf{x} + \lambda\mathbf{c} = 0 \quad \text{and} \quad \mathbf{c}^T\Delta\mathbf{x} = c_0$$

$$\text{or} \quad \begin{bmatrix} \mathbf{H} & \mathbf{c} \\ \mathbf{c}^T & 0 \end{bmatrix} \begin{bmatrix} \Delta\mathbf{x} \\ \lambda \end{bmatrix} = \begin{bmatrix} -\mathbf{g}_0 \\ c_0 \end{bmatrix} \tag{23}$$

Another way of applying linear constraints is the projection method, in which a projector $\mathbf{P}$ is used to remove the directions in which the displacements are constrained to be zero.

$$\mathbf{P}\mathbf{g}_0 + \mathbf{P}\mathbf{H}_0\mathbf{P}\Delta\mathbf{x} + \alpha(\mathbf{I} - \mathbf{P}) = 0,$$

$$\mathbf{P} = \mathbf{I} - \sum_i \mathbf{c}_i\mathbf{c}_i^T/|\mathbf{c}_i|^2, \tag{24}$$

where the $\mathbf{c}_i$ are a set of orthogonal constraint vectors and $\alpha > 0$. For redundant internal coordinates, the projector needs to remove the coordinate redundancies as well as the constraint directions.[58]

SPECIAL CONSIDERATIONS FOR TRANSITION STRUCTURE OPTIMIZATION

Finding a minimum is comparatively easy because the negative of the gradient always points downhill. By contrast, a transition structure optimization must step uphill in one direction and downhill in all other orthogonal directions. Often, the uphill direction is not known in advance and must be determined during the course of the optimization. As a result, numerous special methods have been developed for transition structure searching and many of them are closely related. They can be loosely classified as single-ended and double-ended methods.[2] Single-ended methods start with an initial structure and displace it toward the transition structure. These algorithms include quasi-Newton and related methods (as discussed above and in *Quasi-Newton Methods for Transition Structures* and *Related Single-Ended Methods*). Double-ended methods start from the reactants and products and work from both sides to find the transition structure and the reaction path. These include the nudged elastic band (NEB) method, string method (SM), and growing string method (GSM; see *Chain-of-States and Double-Ended Methods*).

The success of a given transition structure optimization method depends on the topology of the surface as well as the starting structure(s), initial Hessian(s), and coordinates. The two dimensional contour plots in Figure 3 illustrate some of the important features that can be found in higher dimensional surfaces.[112,113] If the change from reactant to product is dominated by a single coordinate, the potential energy surface will have an approximately linear valley, as shown in Figure 3(a). Hindered rotation about a single bond is an example of such an I-shaped surface. All methods should be able to find the transition structure on this type of surface without difficulty. Making one bond and breaking the other results in an L- or V-shaped surface, as shown in Figure 3(b). Because the reaction path is strongly curved, finding the transition structure can be a bit more difficult. A T-shaped surface involves a transition structure

© 2011 John Wiley & Sons, Ltd.

17590884, 2011, 5, Downloaded from https://wires.onlinelibrary.wiley.com/doi/10.1002/wcms.34 by Research Institute for Healthcare Organization and Medical Management of Moscow Healthcare Department, Wiley Online Library on [12/05/2023]. See the Terms and Conditions (https://onlinelibrary.wiley.com/terms-and-conditions) on Wiley Online Library for rules of use; OA articles are governed by the applicable Creative Commons License

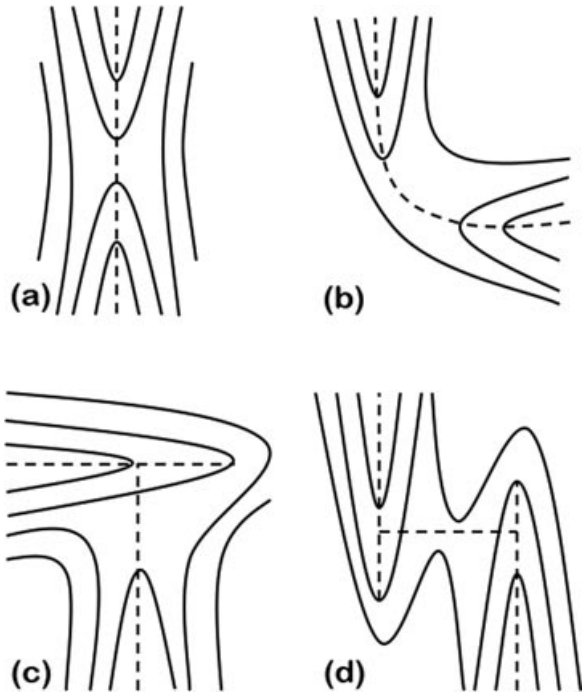

FIGURE 3 | Various classes of reaction channels near the transition structure on reactive potential energy surfaces: (a) I-shaped valley, (b) L- or V-shaped valley, (c) T-shaped valley, and (d) H- or X-shaped valley. (Reprinted with permission from Ref 113. Copyright 2009 ACS Publications.)

in a hanging valley at the side of a main valley, Figure 3(c). A method that follows the main valley will miss the transition structure, but will reach the transition structure if it starts from the other valley. The H- or X-shaped surface in Figure 3(d) is the most difficult because following the valley floor from either the reactant or the product side will miss the transition structure.

Quasi-Newton and single-ended methods are discussed first. These methods differ primarily in the way they try to get close to the quadratic region of transition structure. Double-ended methods start with the reactants and products, and optimize the reaction path as well as the transition structure.

Quasi-newton Methods for Transition Structures

Newton and quasi-Newton algorithms are the most efficient single-ended methods for optimizing transition structures if the starting geometry is within the quadratic region of the transition structure. With suitable techniques for controlling the optimization steps such as TRM, RFO and eigenvector following (see *Step Size Control*), these methods will also converge to a transition structure even if they start outside the quadratic region. Many of the related methods differ primarily in the techniques they use to get close to the quadratic region. There are three main differences in using quasi-Newton methods to optimize transition structures compared with minima:

1. The Hessian update must allow for negative eigenvalues (*Newton and Quasi-Newton Methods*). BFGS (Eq. (7)) yields a positive definite update and is not appropriate. SR1 and PSB updates are suitable (Eqs. (6) and (8)); the Bofill update[74] (Eq. (9)) combines SR1 and PSB yielding better results.
2. Line searches (*Step Size Control*) are generally not possible because the step toward the transition structure may be uphill or downhill. If the coordinates can be partitioned *a priori* into a subspace spanning the coordinates involved in the transition vector and the remaining subspace involving only coordinates to be minimized, then a line search can be used in the latter subspace.
3. Controlling the step size and direction (see *Step Size Control*) are keys to the success of quasi-Newton methods for transition structures, especially if the initial structure is not in the quadratic region. For the TRM (Eq. (18)), the shifted Hessian, $\mathbf{H} - \lambda\mathbf{I}$, is required to have one negative eigenvalue and λ must be chosen so that the step size does not exceed τ. This is illustrated in Figure 2(b) and discussed in the section *Step Size Control*. For the partitioned rational function optimization and eigenvector following methods,[105–109] Eqs. (19) and (20), two different values of λ are used, one to shift the eigenvalue for the maximization direction and the other to shift the eigenvalues for minimization in the remaining directions.

A quasi-Newton optimization of a transition structure requires an initial geometry and an initial estimate of the Hessian. The initial geometry must be somewhere near the quadratic region of the transition structure. This can be challenging at times because our qualitative understanding of transition structure geometries is not as well developed as for equilibrium geometries. There are some general rules-of-thumb that may be useful. For example, the bonds that are being made or broken in a reaction are, in many cases, elongated by ca 50% in the transition structure. The Hammond's postulate[114] is useful for estimating the position of the transition structure along the reaction path. It states that the transition structure

17590884, 2011, 5, Downloaded from https://wires.onlinelibrary.wiley.com/doi/10.1002/wcms.34 by Research Institute for Healthcare Organization and Medical Management of Moscow Healthcare Department, Wiley Online Library on [12/05/2023]. See the Terms and Conditions (https://onlinelibrary.wiley.com/terms-and-conditions) on Wiley Online Library for rules of use; OA articles are governed by the applicable Creative Commons License

is more reactant-like for an exothermic reaction and more product-like for an endothermic reaction. Orbital symmetry/phase conservation rules[115] may indicate when a reaction should occur via a non-least-motion pathway. The choice of coordinates for the optimization is also very important. Often the union between the (redundant) internal coordinates of the reactants and products provides a good coordinate set for the transition structure. Sometimes extra dummy atoms may need to be added to avoid problems with the coordinate system.

When a transition structure for an analogous reaction is not available as an initial guess, then bracketing the search region for the transition structure optimization can be useful. In the QST2 approach,[116] a structure on the reactant side and one on the product side are used to provide bounds on transition structure geometry and to approximate the direction of the reaction path through the transition structure. The QST3 input adds a third structure as an initial estimate of the transition structure. A series of steps is taken along the path connecting these two or three structures until a maximum is reached. Then, a full dimensional quasi-Newton optimization is carried out to find the transition structure.

Quasi-Newton methods require an initial estimate of the Hessian that has a negative eigenvalue with a corresponding eigenvector that is roughly parallel to the desired reaction path. The empirical rules for estimating Hessians for equilibrium geometries[78–80] do not provide suitable estimates of the required negative eigenvalue and eigenvector of the Hessian. Thus, quasi-Newton transition structure optimizations are typically started with an analytical or numerical calculation of the full Hessian (or at least numerical calculation of the most important components of the Hessian needed to obtain the transition vector). For QST*n* methods,[116] updating the Hessian during initial maximization steps along the reaction path is usually sufficient to produce a suitable negative eigenvalue and corresponding eigenvector.

An empirical valence bond (EVB) model[117] of the surface can be useful in obtaining a starting geometry and an initial Hessian for a quasi-Newton transition structure optimization. A quadratic surface is constructed around the reactant minimum and another around the product minimum. These two surfaces intersect along a seam. The lowest point along this seam is a good estimate of the transition structure geometry[118,119] (provided that there are no additional intermediates or transition structures along the reaction path). An initial estimate of the Hessian can be obtained from the interaction of the reactant surface and the product surface using a 2×2 EVB Hamiltonian with a suitable guess for the interaction matrix element.[120]

If more information about the potential energy surface is needed to find the quadratic region of the transition structure, then one can calculate the energy for a series of points along the linear synchronous transit[121] (LST) path between reactants and products to find a maximum along this approximate path (LST scan); internal or distance matrix coordinates are better than Cartesian coordinates for an LST scan. For more complex systems, two or more directions may need to be scanned to find the ridge separating reactants and products. These scans could be carried out with or without optimizing the remaining coordinates (relaxed vs rigid surface scan). The reduced surface method[110,111] selects a set of coordinates to span a two- or three-dimensional surface and minimizes the energy with respect to all of the remaining coordinates. This reduced dimensional surface can be interpolated using distance-weighted interpolants and searched exhaustively for the lowest energy transition structures and reaction paths.

Related Single-Ended Methods

In principle, one should be able to start at the reactants (or products) and go uphill to the transition structure. However, all directions from a minimum are uphill and most will end at higher energy transition structures or higher-order saddle points. One approach is to choose a coordinate that will carry the molecule from reactant to product and step along this coordinate while minimizing all other directions. This is known as coordinate driving and involves a series of constrained optimizations (see *Constrained Optimization*). Coordinate driving has its pitfalls.[122–125] For example, if the dominant coordinate changes along the reaction path, this approach may not work (e.g., Figure 3(c) and (d)). Alternatively, one can choose a direction and perform a constrained optimization of the components of the gradient perpendicular to this direction. This is known variously as line-then-plane,[126] reduced gradient following,[127–129] and Newton trajectories.[130–132] Growing string methods (GSM)[131–136] are coordinate driving or reduced gradient following/Newton trajectory methods that start from both the reactant and product side. Because GSMs are double-ended methods closely related to chain-of-states methods like NEB method and SM; they are discussed in the next section.

An alternative to coordinate driving and reduced gradient following is to step uphill along the lowest eigenvector of the Hessian—this amounts

 © 2011 John Wiley & Sons, Ltd.

17590884, 2011, 5, Downloaded from https://wires.onlinelibrary.wiley.com/doi/10.1002/wcms.34 by Research Institute for Healthcare Organization and Medical Management of Moscow Healthcare Department, Wiley Online Library on [12/05/2023]. See the Terms and Conditions (https://onlinelibrary.wiley.com/terms-and-conditions) on Wiley Online Library for rules of use; OA articles are governed by the applicable Creative Commons License

to the walking up valleys or eigenvector following method described above.[101–109] Stepping toward the transition structure is handled by a quasi-Newton approach with TRM and RFO, Eqs. (18)–(20), to control the step.

The dimer method[137–140] is a variant of the eigenvector following approach that uses gradients calculated at two closely spaced points to keep track of the direction to search for a maximum. At each step, the dimer is rotated to minimize the sum of the two energies (this can be the more costly step in the dimer method). The minimum in the dimer energy occurs when the vector between the points is aligned with the Hessian eigenvector with the lowest eigenvalue. The midpoint of the dimer is displaced uphill toward the transition structure in a manner similar to the eigenvector following method.

Another way to walk uphill along the shallowest ascent path is to follow a gradient extremal path.[141–143] Although steepest descent reaction paths can only be followed downhill, gradient extremal paths are defined locally (the gradient is an eigenvector of the Hessian) and can be followed uphill as well as downhill. A number of algorithms have been developed for following gradient extremal paths.[144–146] Gradient extremals do pass through minima, transition structures, and higher-order saddle points; however, they have a tendency to wander about the surface rather than follow the more direct route that steepest descent paths take.[146,147] This makes gradient extremal path following less attractive for transition structure optimization.

The image function or associated surface approach[148–150] converts a transition structure search into a minimization on a modified surface that has a minimum that coincides with the transition structure of the original function. In a representation in which the Hessian is diagonal, this is accomplished by choosing an eigenvector to follow and inverting the sign of the corresponding component of the gradient and Hessian eigenvalue. A TRM approach, Eq. (18), is then used to search for the minimum on the image function or associated surface. The transition structure can also be optimized as a minimum on the gradient norm surface, $|\mathbf{g}(\mathbf{x})|$ (Refs 151–153); however, the gradient norm can have additional minima at nonstationary points in which the gradient is not zero. Because of the many minima and smaller radius of convergence, minimizing the gradient norm is less practical for transition structure optimizations.

Bounds on the transition structure can be found by approaching it from both the reactant and product side, providing progressively tighter limits.[142,154,155] This is closely related to the GSM[131–136] (see below).

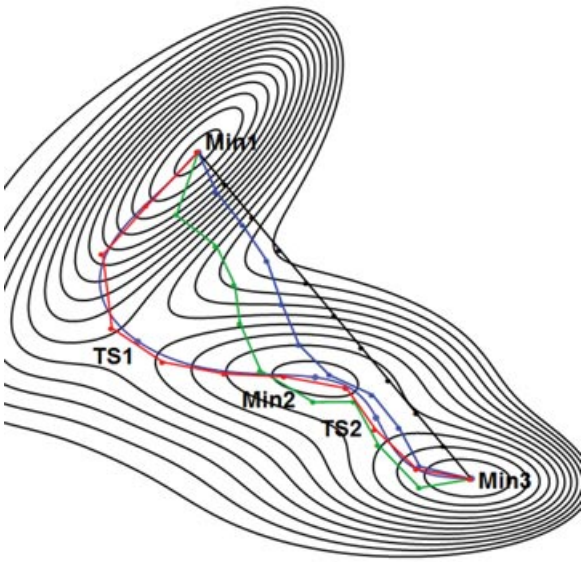

FIGURE 4 | An example of a double-ended reaction path optimization on the Muller–Brown surface.[154] The path optimization with 11 points starts with the linear synchronous transit path (black); the first two iterations are shown in blue and green, respectively. The path after 12 steps is in red and can be compared with the steepest descent path in light blue.

Given two points on opposite sides of the ridge separating reactants from products, the ridge method[156,157] can also be used to optimize the transition structure. A point on the ridge is obtained by finding a maximum along a line connecting a point in the reactant valley and a point in the product valley. Two points on opposite sides of the ridge point are generated by taking small steps along this line. Then, a downhill step is taken from these two points to generate two new points; the maximum along the line between these new points is a lower energy ridge point. The process is repeated until a minimum is found along the ridge; this minimum is a transition structure.

Chain-of-States and Double-Ended Methods

Instead of optimizing a single point toward the transition structure for a reaction, an alternative approach is to optimize the entire reaction path connecting reactants to products. Typically this is done by representing the path by a series of points, that is, a chain-of-states. An example of a path optimization on the Muller–Brown surface[154] is shown in Figure 4. The various methods of this type differ primarily by how the points are generated, what function of the points is minimized, and what constraints are imposed to control the optimization. Many of the path optimization

17590884, 2011, 5, Downloaded from https://wires.onlinelibrary.wiley.com/doi/10.1002/wcms.34 by Research Institute for Healthcare Organization and Medical Management of Moscow Healthcare Department, Wiley Online Library on [12/05/2023]. See the Terms and Conditions (https://onlinelibrary.wiley.com/terms-and-conditions) on Wiley Online Library for rules of use; OA articles are governed by the applicable Creative Commons License

methods are based on minimizing the integral of the energy along the path, normalized by the path length[158]:

$$E^{\text{path}} = \frac{1}{L}\int E(\mathbf{x}(s))\,\mathrm{d}s, \tag{25}$$

where L is the total length of the path. Although this does not yield a steepest descent path,[159] it provides a good approximation to it. The elastic band or chain-of-states method replaces the integral by a discrete set of points, and the path is found by a constrained minimization of the sum of the energies of the points on the path from reactants to products,

$$V^{\text{path}} = \sum E(\mathbf{x}_i), \tag{26}$$

where $\mathbf{x}_i$ are the points on the path, which are required to remain equally spaced. Additional potentials are sometimes introduced to prevent the path from kinking or coiling up in minima.[160] The number of points needed depends on the nature of the path (e.g., number of intermediates and transition states, curvature of the path, etc.) and can range from less than 10 to more than 50. Typically, several thousands of steps are required for convergence, primarily because the motions of adjacent points are strongly coupled. The nudged elastic band (NEB) method[161–170] and string method (SM)[171–176] are two current approaches that offer some improvement in the convergence of the path optimization.

In the NEB method,[161–163] the points are kept equally spaced by adding a spring potential between the points (c.f. penalty function method, *Constrained Optimization*):

$$V^{\text{spring}} = \frac{1}{2}k^{\text{spring}}\sum(\mathbf{x}_i - \mathbf{x}_{i-1})^2. \tag{27}$$

The gradient for a point has contributions from the potential energy surface and from the spring potential, which can be projected into components parallel and perpendicular to the path:

$$\mathbf{g}_i = \frac{\mathrm{d}V^{\text{path}}}{\mathrm{d}\mathbf{x}_i} \quad \mathbf{g}_i^{\parallel} = \left(\mathbf{g}_i^T\boldsymbol{\tau}_i\right)\boldsymbol{\tau}_i \quad \mathbf{g}_i^{\perp} = \mathbf{g}_i - \mathbf{g}_i^{\parallel}, \tag{28}$$

$$\tilde{\mathbf{g}}_i = \frac{\mathrm{d}V^{\text{spring}}}{\mathrm{d}\mathbf{x}_i} \quad \tilde{\mathbf{g}}_i^{\parallel} = \left(\tilde{\mathbf{g}}_i^T\boldsymbol{\tau}_i\right)\boldsymbol{\tau}_i \quad \tilde{\mathbf{g}}_i^{\perp} = \tilde{\mathbf{g}}_i - \tilde{\mathbf{g}}_i^{\parallel}, \tag{29}$$

where $\boldsymbol{\tau}_i$ is the normalized tangent to the path at $\mathbf{x}_i$. The tangent can be calculated by central difference (of $\mathbf{x}_{i-1}$ and $\mathbf{x}_{i+1}$) or by forward difference using the point uphill from $\mathbf{x}_i$. The NEB method[161–163] uses the gradient of the spring potential to displace (nudge) the points along the reaction path, and uses the gradient of the unmodified potential energy surface for directions perpendicular to the path.

$$\mathbf{g}_i^{\text{NEB}} = \mathbf{g}_i^{\perp} + \tilde{\mathbf{g}}_i^{\parallel} \tag{30}$$

The doubly NEB method[164] includes a portion of the spring gradient perpendicular to the path (e.g., a second nudge).

$$\mathbf{g}_i^{DNEB} = \mathbf{g}_i^{\perp} + \tilde{\mathbf{g}}_i^{\parallel} + \left(\tilde{\mathbf{g}}_i^{\perp} - \left(\tilde{\mathbf{g}}_i^{\perp T}\mathbf{g}_i^{\perp}\right)\mathbf{g}_i^{\perp}/|\mathbf{g}_i^{\perp}|^2\right) \tag{31}$$

This accelerates the optimization in the early stages, but may inhibit full convergence in the later stages.[168]

The original NEB method used a quenched or damped Velocity Verlet method to propagate the points toward the path.[161–163] After each step, most of the velocity is removed. Alternatively, a quasi-Newton method can be used for the constrained optimization, preferably by moving all of the points simultaneously.[164,165,167,168] Because the dimension of the optimization problem (number of coordinate times the number of points) can be rather large, limited memory quasi-Newton methods such as L-BFGS and ABNR have been used.[164,165,167,168] Currently, the NEB/L-BFGS method is the most efficient and stable nudge elastic band method.[168]

The spring potential used to maintain uniform spacing in the NEB method introduces additional coupling between the points on the path that slows down the convergence of the optimization. An early path optimization method avoided the spring potential by moving the points so that the gradient would lie on the steepest descent path.[173] The recently developed string method[171,172] also minimizes the perpendicular gradient, $\mathbf{g}_i^{\perp}$ in Eq. (28), for the points on the path. A cubic spline is used to redistribute the points to maintain equal spacing and the fourth-order Runge–Kutta method is used to evolve the path.[171,172] In the quadratic string method, the points move on local quadratic approximations to the surface using updated Hessians.[174,175] Alternatively, the L-BFGS method can be used to propagate all of the points at the same time.[168] The efficiency of the best string methods appears to be similar to the best NEB methods, requiring from hundreds to thousands of gradient calculations to optimize the path.[168,176]

The GSM[133–136] reduces the total effort by generating the points one at a time starting from the reactants and products. This is similar to the line-then-plane method[126] and reduced gradient following/Newton trajectories[131,132] from both ends of the path. The GSM is also closely related to earlier methods that stepped from the reactant and product toward the transition structure.[142,154,155] As the string grows toward the center, the endpoints of the string provide better brackets for the transition structure. The search can be completed by interpolating to the

© 2011 John Wiley & Sons, Ltd.

17590884, 2011, 5, Downloaded from https://wires.onlinelibrary.wiley.com/doi/10.1002/wcms.34 by Research Institute for Healthcare Organization and Medical Management of Moscow Healthcare Department, Wiley Online Library on [12/05/2023]. See the Terms and Conditions (https://onlinelibrary.wiley.com/terms-and-conditions) on Wiley Online Library for rules of use; OA articles are governed by the applicable Creative Commons License

maximum along the path and optimizing the transition structure.[136] If the ends of the growing string are too far apart, a NEB method or SM can be used to optimize of the entire path. To reduce the cost, a low level of theory can be used to grow the string and a higher level of theory can be used to refine the string or to optimize the transition structure.[134,135]

Chain-of-state methods such as NEB, SM, and GSM are still more costly than quasi-Newton methods for transition structures, and there is considerable room for improving the efficiency of these methods. However, these methods do map out the entire reaction path. This can be advantageous if the path contains several transition states and intermediates. Furthermore, chain-of-states methods are more readily parallelized than quasi-Newton and other single-ended methods. The development of these methods is ongoing.

Characterization of an Optimized Transition Structures

Once a transition structure has been optimized, it is necessary to confirm that it is indeed a transition structure and is appropriate for the reaction under consideration. A vibrational frequency calculation needs to be carried out for the transition structure to confirm that it has one and only one imaginary frequency (equivalently, the full dimensional Hessian must have one and only one negative eigenvalue). It is not sufficient to examine the updated Hessian used in the quasi-Newton optimization process because it may be subject to numerical noise and the optimization may not have explored the full coordinate space (e.g., modes that lower the symmetry of the molecule). Firstly, an accurate Hessian must be calculated analytically or numerically and used for the vibrational frequency analysis. Secondly, the transition vector, that is, the vibrational normal mode associated with the imaginary frequency must be inspected to make sure that the motion corresponds to the desired reaction. This is most easily done with graphical software that can animate vibrational modes. For complex reaction networks, reaction path following may be needed to verify that the transition structure connects the desired reactants and products. Chain-of-states methods yield good approximations to the reaction path as a part of the optimization. For quasi-Newton and other methods that converge on a single structure, following the steepest descent path (see *Reaction Path Following*) will indicate the reactants and products connected by the transition structure. Reaction path following may also reveal other stationary points on the path.

REACTION PATH FOLLOWING

For quasi-Newton and related methods that locate only the transition structure, the steepest descent reaction path can be obtained by following the gradient downhill. Chain-of-states approaches such as NEB method, SM, and GMS (see *Chain-of-States and Double-Ended Methods*) provide an approximation to the reaction path as a part of the optimization. Methods such as variational transition state theory[177] and reaction path Hamiltonian[178] may require a more accurate path. For this case, rather than trying to obtain very tight convergence with a chain-of-states method, it is much more efficient to calculate an accurate path by a reaction path following method.

In the steepest descent reaction path (SDP) or minimum energy path (MEP), $\mathbf{x}(s)$ is defined as:

$$\frac{d\mathbf{x}(s)}{ds} = \frac{-\mathbf{g}(\mathbf{x}(s))}{|\mathbf{g}(\mathbf{x}(s))|}, \tag{32}$$

where s is the arc length along the path. When mass-weighted coordinates are used, the path is the IRC of Fukui[179] and corresponds to a classical particle moving with infinitesimal kinetic energy. A number of reviews are available for reaction path following methods.[8,180] In principle, the reaction path can be obtained by standard methods for numerical integration of ordinary differential equations.[181] However, in some regions of the potential energy surface, these methods produce paths that zigzag across the valley unless very small step sizes are used. This is characteristic of stiff differential equations for which special techniques such as implicit methods are needed.[182]

The Ishida, Morokuma, Komornicki (IMK) method[183] uses an Euler step followed by a line search to step back toward the path. The LQA method of McIver and Page,[184,185] and subsequent improvements by others[186–188] obtain a step along the path by integrating Eq. (32) analytically on a quadratic energy surface using a calculated or updated Hessian. Because it makes use of quadratic information, LQA can take large steps than IMK. The second-order method of Gonzalez and Schlegel[189,190] (GS2) is an implicit trapezoid method that combines an explicit Euler step with an implicit Euler step. The latter is obtained by a constrained optimization. The larger step size and greater stability of the GS2 method more than compensates for the few extra gradient calculations needed in the optimization. The implicit trapezoid method has been generalized and extended by Burger and Yang[191,192] to a family of implicit–explicit methods for accurate and efficient integration of reaction paths.

 © 2011 John Wiley & Sons, Ltd.

17590884, 2011, 5, Downloaded from https://wires.onlinelibrary.wiley.com/doi/10.1002/wcms.34 by Research Institute for Healthcare Organization and Medical Management of Moscow Healthcare Department, Wiley Online Library on [12/05/2023]. See the Terms and Conditions (https://onlinelibrary.wiley.com/terms-and-conditions) on Wiley Online Library for rules of use; OA articles are governed by the applicable Creative Commons License

The reaction path can be thought of as an average over a collection of classical trajectories or a trajectory in a very viscous medium. The dynamic reaction path method[193] and the damped Velocity Verlet approach[194] obtain a reaction path by calculating a classical trajectory in which almost all of the kinetic energy has been removed at every step. The Hessian-based predictor–corrector method for reaction paths[195,196] adapts an algorithm used for classical trajectory calculations. An LQA predictor step is taken on a local quadratic surface; a new Hessian is obtained at the end of the predictor step (by updating or by direct calculation); a corrector step is obtained on a distance-weighted interpolant using the local quadratics at the beginning and end of the predictor step.

A reaction path calculated at a lower level of theory can be used to provide an estimate of the transition structure optimization at a higher level of theory when full optimization at the higher level is not practical. The potential energy surface is more likely to change along the path than perpendicular to the path because reaction energies and bond making/breaking coordinates are typically more sensitive to the accuracy of the electronic structure calculation. In the IRCMax method, single point high-level energy calculations along the low-level path are interpolated to give an estimate of the transition structure and energy at the high level of theory.[197]

Reaction paths can also be formulated as a variational method by finding the path that minimizes the following integral[159,198–201]:

$$I = \int \sqrt{\mathbf{g}(\mathbf{x}(t))^T\, \mathbf{g}(\mathbf{x}(t))}\, \sqrt{(\mathrm{d}\mathbf{x}(t)/\mathrm{d}t)^T(\mathrm{d}\mathbf{x}(t)/\mathrm{d}t)}\, \mathrm{d}t$$
$$= \int \sqrt{\mathbf{g}(\mathbf{x}(s))^T\, \mathbf{g}(\mathbf{x}(s))}\, \mathrm{d}s, \qquad (33)$$

where $\mathbf{x}(t)$ is the reaction path parameterized by an arbitrary variable t, whereas $\mathbf{x}(s)$ is the reaction path as a function of the arc length (see Eq. (32)). This is closely related to obtaining a classical trajectory by finding the path that minimizes the classical action, and may hold promise for future developments.

SUMMARY

Methods for optimizing equilibrium geometries, locating transition structures, and following reaction paths have been outlined in this chapter. Quasi-Newton methods are very efficient for geometry optimization when used with Hessian updating, approximate line searches, and trust radius or rational function techniques for step size control. Single-ended and double-ended methods for transition structure searches have been summarized. Procedures for approaching transitions structures are described. Quasi-Newton methods with eigenvector following and rational function optimization are efficient for finding transition structures. Double-ended techniques for transition structures are discussed and include nudged elastic band, string and growing string methods. The chapter concludes with a discussion of validating transition structures and a description of methods for following steepest descent paths.

REFERENCES

1. Hratchian HP, Schlegel HB. Finding minima, transition states, and following reaction pathways on *ab initio* potential energy surfaces. In: Dykstra CE, Frenking G, Kim KS, Scuseria GE, eds. *Theory and Applications of Computational Chemistry: the First Forty Years*. New York: Elsevier; 2005, 195–249.
2. Wales DJ. *Energy Landscapes*. Cambridge: Cambridge University Press; 2003.
3. Schlegel HB. Exploring potential energy surfaces for chemical reactions: an overview of some practical methods. *J Comput Chem* 2003, 24:1514–1527.
4. Pulay P, Baker J. Optimization and reaction path algorithms. In: Spencer ND, Moore JH, eds. *Encyclopedia of Chemical Physics and Physical Chemistry*. Bristol: Institute of Physics; 2001, 2061–2085.
5. Schlegel HB. Geometry optimization. In: Schleyer PvR, Allinger NL, Kollman PA, Clark T, Schaefer HF III, Gasteiger J, Schreiner PR, eds. *Encyclopedia of Computational Chemistry*. Vol 2. Chichester: John Wiley & Sons; 1998, 1136–1142.
6. Schlick T. Geometry optimization: 2. In: Schleyer PvR, Allinger NL, Kollman PA, Clark T, Schaefer HF III, Gasteiger J, Schreiner PR, eds. *Encyclopedia of Computational Chemistry*. Vol 2. Chichester: John Wiley & Sons; 1998: 1142–1157.
7. Jensen F. Transition structure optimization techniques. In: Schleyer PvR, Allinger NL, Kollman PA, Clark T, Schaefer HF III, Gasteiger J, Schreiner PR, eds. *Encyclopedia of Computational Chemistry*. Vol 5. Chichester: John Wiley & Sons; 1998: 3114–3123.

 © 2011 John Wiley & Sons, Ltd.

17590884, 2011, 5, Downloaded from https://wires.onlinelibrary.wiley.com/doi/10.1002/wcms.34 by Research Institute for Healthcare Organization and Medical Management of Moscow Healthcare Department, Wiley Online Library on [12/05/2023]. See the Terms and Conditions (https://onlinelibrary.wiley.com/terms-and-conditions) on Wiley Online Library for rules of use; OA articles are governed by the applicable Creative Commons License

8. Schlegel HB. Reaction path following. In: Schleyer PvR, Allinger NL, Kollman PA, Clark T, Schaefer HF III, Gasteiger J, Schreiner PR, eds. *Encyclopedia of Computational Chemistry*. Vol 4. Chichester: John Wiley & Sons; 1998: 2432–2437.
9. Schlegel HB. Geometry optimization on potential energy surfaces. In: Yarkony DR, ed. *Modern Electronic Structure Theory*. Singapore: World Scientific Publishing; 1995, 459–500.
10. Liotard DA. Algorithmic tools in the study of semiempirical potential surfaces. *Int J Quantum Chem* 1992, 44:723–741.
11. Schlegel HB. Some practical suggestions for optimizing geometries and locating transition states. In: Bertrán J, ed. *New Theoretical Concepts for Understanding Organic Reactions*. Vol 267. The Netherlands: Kluwer Academic; 1989, 33–53.
12. Head JD, Weiner B, Zerner MC. A survey of optimization procedures for stable structures and transition-states. *Int J Quantum Chem* 1988, 33:177–186.
13. Schlegel HB. Optimization of equilibrium geometries and transition structures. *Adv Chem Phys* 1987, 67:249–286.
14. Bell S, Crighton JS. Locating transition-states. *J Chem Phys* 1984, 80:2464–2475.
15. Jensen F. *Introduction to Computational Chemistry*. Chichester; NY: John Wiley & Sons; 2007.
16. Cramer CJ. *Essentials of Computational Chemistry: Theories and Models*. West Sussex, New York: John Wiley & Sons; 2004.
17. Gill PE, Murray W, Wright MH. *Practical Optimization*. London, New York: Academic Press; 1981.
18. Dennis JE, Schnabel RB. *Numerical Methods for Unconstrained Optimization and Nonlinear Equations*. Englewood Cliffs, NJ: Prentice-Hall; 1983.
19. Scales LE. *Introduction to Non-Linear Optimization*. New York: Springer-Verlag; 1985.
20. Fletcher R. *Practical Methods of Optimization*. 2nd ed. Chichester: John Wiley & Sons; 1987.
21. Maeda S, Ohno K, Morokuma K. An automated and systematic transition structure explorer in large flexible molecular systems based on combined global reaction route mapping and microiteration methods. *J Chem Theory Comput* 2009, 5:2734–2743.
22. Maeda S, Ohno K, Morokuma K. Automated global mapping of minimal energy points on seams of crossing by the anharmonic downward distortion following method: a case study of H2CO. *J Phys Chem A* 2009, 113:1704–1710.
23. E W, Vanden-Eijnden E. Transition path theory and path finding algorithms for the study of rare events. *Annu Rev Phys Chem* 2010, 61:391–420.
24. Koga N, Morokuma K. Determination of the lowest energy point on the crossing seam between two potential surfaces using the energy gradient. *Chem Phys Lett* 1985, 119:371–374.
25. Farazdel A, Dupuis M. On the determination of the minimum on the crossing seam of two potential energy surfaces. *J Comput Chem* 1991, 12:276–282.
26. Ragazos IN, Robb MA, Bernardi F, Olivucci M. Optimization and characterization of the lowest energy point on a conical intersection using an MCSCF Larangian. *Chem Phys Lett* 1992, 197:217–223.
27. Manaa MR, Yarkony DR. On the intersection of two potential energy surfaces of the same symmetry. Systematic characterization using a Lagrange multiplier constrained procedure. *J Chem Phys* 1993, 99:5251–5256.
28. Bearpark MJ, Robb MA, Schlegel HB. A direct method for the location of the lowest energy point on a potential surface crossing. *Chem Phys Lett* 1994, 223:269–274.
29. Anglada JM, Bofill JM. A reduced-restricted-quasi-Newton-Raphson method for locating and optimizing energy crossing points between two potential energy surfaces. *J Comput Chem* 1997, 18:992–1003.
30. De Vico L, Olivucci M, Lindh R. New general tools for constrained geometry optimizations. *J Chem Theory Comput* 2005, 1:1029–1037.
31. Levine BG, Ko C, Quenneville J, Martinez TJ. Conical intersections and double excitations in time-dependent density functional theory. *Mol Phys* 2006, 104:1039–1051.
32. Keal TW, Koslowski A, Thiel W. Comparison of algorithms for conical intersection optimisation using semiempirical methods. *Theor Chem Acc* 2007, 118:837–844.
33. Bearpark MJ, Larkin SM, Vreven T. Searching for conical intersections of potential energy surfaces with the ONIOM method: application to previtamin D. *J Phys Chem A* 2008, 112:7286–7295.
34. Sicilia F, Blancafort L, Bearpark MJ, Robb MA. New algorithms for optimizing and linking conical intersection points. *J Chem Theory Comp* 2008, 4:257–266.
35. Dick B. Gradient projection method for constraint optimization and relaxed energy paths on conical intersection spaces and potential energy surfaces. *J Chem Theory Comput* 2009, 5:116–125.
36. Madsen S, Jensen F. Locating seam minima for macromolecular systems. *Theor Chem Acc* 2009, 123:477–485.
37. Bakken V, Helgaker T. The efficient optimization of molecular geometries using redundant internal coordinates. *J Chem Phys* 2002, 117:9160–9174.

17590884, 2011, 5, Downloaded from https://wires.onlinelibrary.wiley.com/doi/10.1002/wcms.34 by Research Institute for Healthcare Organization and Medical Management of Moscow Healthcare Department, Wiley Online Library on [12/05/2023]. See the Terms and Conditions (https://onlinelibrary.wiley.com/terms-and-conditions) on Wiley Online Library for rules of use; OA articles are governed by the applicable Creative Commons License

38. Baker J. Techniques for geometry optimization: a comparison of cartesian and natural internal coordinates. *J Comput Chem* 1993, 14:1085–1100.
39. Baker J, Chan FR. The location of transition states: a comparison of Cartesian, Z-matrix, and natural internal coordinates. *J Comput Chem* 1996, 17:888–904.
40. McQuarrie DA. *Statistical Thermodynamics*. Mill Valley, CA: University Science Books; 1973.
41. Heidrich D. *The Reaction Path in Chemistry: Current Approaches and Perspectives*. Dordrecht: Kluwer; 1995.
42. Haile JM. *Molecular Dynamics Simulation: Elementary Methods*. New York: John Wiley & Sons; 1992.
43. Thompson DL. Trajectory simulations of molecular collisions: classical treatment. In: Schleyer PvR, Allinger NL, Kollman PA, Clark T, Schaefer HF III, Gasteiger J, Schreiner PR, eds. *Encyclopedia of Computational Chemistry*. Vol 5. Chichester: John Wiley & Sons; 1998, 3056–3073.
44. Hase WL, ed. *Advances in Classical Trajectory Methods*. Greenwich: JAI Press; 1992.
45. Bunker DL. Classical trajectory methods. *Methods Comput Phys* 1971, 10:287.
46. Lasorne B, Worth GA, Robb MA. Excited-state dynamics. *WIREs Comput Mol Sci* 2011, 1:460–475.
47. Wilson EB, Decius JC, Cross PC. *Molecular Vibrations: the Theory of Infrared and Raman Vibrational Spectra*. New York: Dover Publications; 1980.
48. Kolda TG, Lewis RM, Torczon V. Optimization by direct search: new perspectives on some classical and modern methods. *SIAM Rev* 2003, 45:385–482.
49. Garcia-Palomares UM, Rodriguez JF. New sequential and parallel derivative-free algorithms for unconstrained minimization. *SIAM J Optim* 2002, 13:79–96.
50. Lewis RM, Torczon V, Trosset MW. Direct search methods: then and now. *J Comput Appl Math* 2000, 124:191–207.
51. Han LX, Neumann M. Effect of dimensionality on the Nelder–Mead simplex method. *Optim Math Software* 2006, 21:1–16.
52. Hehre WJ, Radom L, Schleyer PvR, Pople JA. *Ab Initio Molecular Orbital Theory*. New York: John Wiley & Sons; 1986.
53. Pulay P, Fogarasi G. Geometry optimization in redundant internal coordinates. *J Chem Phys* 1992, 96:2856–2860.
54. Fogarasi G, Zhou XF, Taylor PW, Pulay P. The calculation of *ab initio* molecular geometries: efficient optimization by natural internal coordinates and empirical correction by offset forces. *J Am Chem Soc* 1992, 114:8191–8201.
55. Baker J, Kessi A, Delley B. The generation and use of delocalized internal coordinates in geometry optimization. *J Chem Phys* 1996, 105:192–212.
56. Baker J, Kinghorn D, Pulay P. Geometry optimization in delocalized internal coordinates: an efficient quadratically scaling algorithm for large molecules. *J Chem Phys* 1999, 110:4986–4991.
57. von Arnim M, Ahlrichs R. Geometry optimization in generalized natural internal coordinates. *J Chem Phys* 1999, 111:9183–9190.
58. Peng CY, Ayala PY, Schlegel HB, Frisch MJ. Using redundant internal coordinates to optimize equilibrium geometries and transition states. *J Comput Chem* 1996, 17:49–56.
59. Farkas Ö, Schlegel HB. Methods for geometry optimization of large molecules. I. An $O(N^2)$ algorithm for solving systems of linear equations for the transformation of coordinates and forces. *J Chem Phys* 1998, 109:7100–7104.
60. Farkas Ö, Schlegel HB. Geometry optimization methods for modeling large molecules. *THEOCHEM* 2003, 666:31–39.
61. Baker J, Pulay P. Geometry optimization of atomic microclusters using inverse-power distance coordinates. *J Chem Phys* 1996, 105:11100–11107.
62. Eckert F, Pulay P, Werner HJ. *Ab initio* geometry optimization for large molecules. *J Comput Chem* 1997, 18:1473–1483.
63. Baker J, Pulay P. Efficient geometry optimization of molecular clusters. *J Comput Chem* 2000, 21:69–76.
64. Billeter SR, Turner AJ, Thiel W. Linear scaling geometry optimisation and transition state search in hybrid delocalised internal coordinates. *Phys Chem Chem Phys* 2000, 2:2177–2186.
65. Paizs B, Baker J, Suhai S, Pulay P. Geometry optimization of large biomolecules in redundant internal coordinates. *J Chem Phys* 2000, 113:6566–6572.
66. Kudin KN, Scuseria GE, Schlegel HB. A redundant internal coordinate algorithm for optimization of periodic systems. *J Chem Phys* 2001, 114:2919–2923.
67. Bucko T, Hafner J, Angyan JG. Geometry optimization of periodic systems using internal coordinates. *J Chem Phys* 2005, 122:124508.
68. Doll K, Dovesi R, Orlando R. Analytical Hartree-Fock gradients with respect to the cell parameter: systems periodic in one and two dimensions. *Theor Chem Acc* 2006, 115:354–360.
69. Murtagh BA, Sargent RWH. Computational experience with quadratically convergent minimization methods. *Comput J* 1972, 13:185–194.
70. Broyden CG. The convergence of a class of double rank minimization algorithms. *J Inst Math Appl* 1970, 6:76–90.
71. Fletcher R. A new approach to variable metric algorithms. *Comput J* 1970, 13:317–322.
72. Goldfarb D. A family of variable metric methods derived by variational means. *Math Comput* 1970, 24:23–26.

 © 2011 John Wiley & Sons, Ltd.

17590884, 2011, 5, Downloaded from https://wires.onlinelibrary.wiley.com/doi/10.1002/wcms.34 by Research Institute for Healthcare Organization and Medical Management of Moscow Healthcare Department, Wiley Online Library on [12/05/2023]. See the Terms and Conditions (https://onlinelibrary.wiley.com/terms-and-conditions) on Wiley Online Library for rules of use; OA articles are governed by the applicable Creative Commons License

73. Shanno DF. Conditioning of quasi-Newton methods for functional minimization. *Math Comput* 1970, 24:647–657.
74. Bofill JM. Updated Hessian matrix and the restricted step method for locating transition structures. *J Comput Chem* 1994, 15:1–11.
75. Farkas Ö, Schlegel HB. Methods for optimizing large molecules. II. Quadratic search. *J Chem Phys* 1999, 111:10806–10814.
76. Bofill JM. Remarks on the updated Hessian matrix methods. *Int J Quantum Chem* 2003, 94:324–332.
77. Liang W, Wang H, Hung J, Li XS, Frisch MJ. Eigenspace update for molecular geometry optimization in nonredundant internal coordinates. *J Chem Theor Comp* 2010, 6:2034–2039.
78. Schlegel HB. Estimating the Hessian for gradient-type geometry optimizations. *Theor Chim Acta* 1984, 66:333–340.
79. Wittbrodt JM, Schlegel HB. Estimating stretching force constants for geometry optimization. *THEOCHEM* 1997, 398:55–61.
80. Fischer TH, Almlof J. General methods for geometry and wave-function optimization. *J Phys Chem* 1992, 96:9768–9774.
81. Nocedal J. Updating quasi-Newton matrices with limited storage. *Math Comput* 1980, 35:773–782.
82. Byrd RH, Lu PH, Nocedal J, Zhu CY. A limited memory algorithm for bound constrained optimization. *SIAM J Sci Comput* 1995, 16:1190–1208.
83. Liu DC, Nocedal J. On the limited memory BFGS method for large-scale optimization. *Math Program* 1989, 45:503–528.
84. Biegler LT, Nocedal J, Schmid C. A reduced Hessian method for large-scale constrained optimization. *SIAM J Optim* 1995, 5:314–347.
85. Morales JL, Nocedal J. Enriched methods for large-scale unconstrained optimization. *Comput Optim Appl* 2002, 21:143–154.
86. Fletcher R. An Optimal positivedefinite update for sparse Hessian matrices. *SIAM J Optim* 1995, 5:192–218.
87. Byrd RH, Nocedal J, Schnabel RB. Representations of quasi-Newton matrices and their use in limited memory methods. *Math Program* 1994, 63:129–156.
88. Anglada JM, Besalu E, Bofill JM. Remarks on large-scale matrix diagonalization using a Lagrange-Newton-Raphson minimization in a subspace. *Theor Chem Acc* 1999, 103:163–166.
89. Prat-Resina X, Garcia-Viloca M, Monard G, Gonzalez-Lafont A, Lluch JM, Bofill JM, Anglada JM. The search for stationary points on a quantum mechanical/molecular mechanical potential energy surface. *Theor Chem Acc* 2002, 107:147–153.
90. Fletcher R, Reeves CM. Function minimization by conjugate gradients. *Comput J* 1964, 7:149–154.
91. Polak E. *Computational Methods in Optimiztion: a Unified Approach*. New York: Academic; 1971.
92. Csaszar P, Pulay P. Geometry optimization by direct inversion in the iterative subspace. *J Mol Struct* 1984, 114:31–34.
93. Farkas Ö. PhD (Csc) thesis. Budapest: Eötvös Loránd University and Hungarian Academy of Sciences; 1995.
94. Farkas Ö, Schlegel HB. Methods for optimizing large molecules. III. An improved algorithm for geometry optimization using direct inversion in the iterative subspace (GDIIS). *Phys Chem Chem Phys* 2002, 4:11–15.
95. Li XS, Frisch MJ. Energy-represented direct inversion in the iterative subspace within a hybrid geometry optimization method. *J Chem Theory Comput* 2006, 2:835–839.
96. Saad Y, Schultz MH. GMRES: a generalized minimal residual algorithm for solving nonsymmetric linear systems. *SIAM J Sci Stat Comput* 1986, 7:856–869.
97. Krylov AN. On the numerical solution of the equation by which in technical questions frequencies of small oscillations of material systems are determined. *Izvestiya Akademii Nauk SSSR, Otdel Mat i Estest Nauk* 1931, 7:491–539.
98. Lanczos C. Solution of systems of linear euations by minimized iterations. *J Res Nat Bur Stand* 1952, 49:33–53.
99. Arnoldi WE. The principle of minimized iterations in the solution of the matrix eigenvalue problem. *Q Appl Math* 1951, 9:17–29.
100. Schlegel HB. Optimization of equilibrium geometries and transition structures. *J Comput Chem* 1982, 3:214–218.
101. Cerjan CJ, Miller WH. On finding transition states. *J Chem Phys* 1981, 75:2800–2806.
102. Simons J, Jorgensen P, Taylor H, Ozment J. Walking on potential energy surfaces. *J Phys Chem* 1983, 87:2745–2753.
103. Nichols J, Taylor H, Schmidt P, Simons J. Walking on potential energy surfaces. *J Chem Phys* 1990, 92:340–346.
104. Simons J, Nichols J. Strategies for walking on potential energy surfaces using local quadratic approximations. *Int J Quantum Chem* 1990, 38(suppl 24):263–276.
105. Banerjee A, Adams N, Simons J, Shepard R. Search for stationary points on surface. *J Phys Chem* 1985, 89:52–57.
106. Baker J. An algorithm for the location of transition states. *J Comput Chem* 1986, 7:385–395.

17590884, 2011, 5, Downloaded from https://wires.onlinelibrary.wiley.com/doi/10.1002/wcms.34 by Research Institute for Healthcare Organization and Medical Management of Moscow Healthcare Department, Wiley Online Library on [12/05/2023]. See the Terms and Conditions (https://onlinelibrary.wiley.com/terms-and-conditions) on Wiley Online Library for rules of use; OA articles are governed by the applicable Creative Commons License

107. Culot P, Dive G, Nguyen VH, Ghuysen JM. A quasi-Newton algorithm for first-order saddle-point location. *Theor Chim Acta* 1992, 82:189–205.
108. Besalu E, Bofill JM. On the automatic restricted-step rational-function-optimization method. *Theor Chem Acc* 1998, 100:265–274.
109. Anglada JM, Bofill JM. On the restricted step method coupled with the augmented Hessian for the search of stationary points of any continuous function. *Int J Quantum Chem* 1997, 62:153–165.
110. Bofill JM, Anglada JM. Finding transition states using reduced potential energy surfaces. *Theor Chem Acc* 2001, 105:463–472.
111. Burger SK, Ayers PW. Dual grid methods for finding the reaction path on reduced potential energy surfaces. *J Chem Theory Comput* 2010, 6:1490–1497.
112. Shaik SS, Schlegel HB, Wolfe S. *Theoretical Aspects of Physical Organic Chemistry: the SN2 Mechanism*. New York: John Wiley & Sons; 1992.
113. Sonnenberg JL, Wong KF, Voth GA, Schlegel HB. Distributed Gaussian valence bond surface derived from *ab initio* calculations. *J Chem Theory Comput* 2009, 5:949–961.
114. Hammond GS. A correlation of reaction rates. *J Am Chem Soc* 1955, 77:334–338.
115. Woodward RB, Hoffmann R. *The Conservation of Orbital Symmetry*. Weinheim/Bergstr.: Verlag Chemie; 1970.
116. Peng CY, Schlegel HB. Combining synchronous transit and quasi-Newton methods to find transition states. *Isr J Chem* 1993, 33:449–454.
117. Warshel A, Weiss RM. An empirical valence bond approach for comparing reactions in solutions and in enzymes. *J Am Chem Soc* 1980, 102:6218–6226.
118. Jensen F. Transition structure modeling by intersecting potential energy surfaces. *J Comput Chem* 1994, 15:1199–1216.
119. Ruedenberg K, Sun JQ. A simple prediction of approximate transition states on potential energy surfaces. *J Chem Phys* 1994, 101:2168–2174.
120. Anglada JM, Besalu E, Bofill JM, Crehuet R. Prediction of approximate transition states by Bell–Evans–Polanyi principle: I. *J Comput Chem* 1999, 20:1112–1129.
121. Halgren T, Lipscomb WN. The synchronous-transit method for determining reaction pathways and locating molecular transition states. *Chem Phys Lett* 1977, 49:225–232.
122. Burkert U, Allinger NL. Pitfalls in the use of the torsion angle driving method for the calculation of conformational interconversions. *J Comput Chem* 1982, 3:40–46.
123. Williams IH, Maggiora GM. Use and abuse of the distinguished coordinate method for transition state structure searching. *THEOCHEM* 1982, 6:365–378.
124. Scharfenberg P. Theoretical analysis of constrained minimum energy paths. *Chem Phys Lett* 1981, 79:115–117.
125. Rothman MJ, Lohr LL. Analysis of an energy minimization method for locating transition states on potential energy hypersurfaces. *Chem Phys Lett* 1980, 70:405–409.
126. Cardenas-Lailhacar C, Zerner MC. Searching for transition states: the line-then-plane (LTP) approach. *Int J Quantum Chem* 1995, 55:429–439.
127. Quapp W, Hirsch M, Imig O, Heidrich D. Searching for saddle points of potential energy surfaces by following a reduced gradient. *J Comput Chem* 1998, 19:1087–1100.
128. Hirsch M, Quapp W. Improved RGF method to find saddle points. *J Comput Chem* 2002, 23:887–894.
129. Crehuet R, Bofill JM, Anglada JM. A new look at the reduced-gradient-following path. *Theor Chem Acc* 2002, 107:130–139.
130. Quapp W. Newton trajectories in the curvilinear metric of internal coordinates. *J Math Chem* 2004, 36:365–379.
131. Quapp W. A growing string method for the reaction pathway defined by a Newton trajectory. *J Chem Phys* 2005, 122:174106.
132. Quapp W. The growing string method for flows of Newton trajectories by a second order method. *J Theor Comput Chem* 2009, 8:101–117.
133. Peters B, Heyden A, Bell AT, Chakraborty A. A growing string method for determining transition states: comparison to the nudged elastic band and string methods. *J Chem Phys* 2004, 120:7877–7886.
134. Goodrow A, Bell AT, Head-Gordon M. Development and application of a hybrid method involving interpolation and *ab initio* calculations for the determination of transition states. *J Chem Phys* 2008, 129:174109.
135. Goodrow A, Bell AT, Head-Gordon M. Transition state-finding strategies for use with the growing string method. *J Chem Phys* 2009, 130:244108.
136. Goodrow A, Bell AT, Head-Gordon M. A strategy for obtaining a more accurate transition state estimate using the growing string method. *Chem Phys Lett* 2010, 484:392–398.
137. Henkelman G, Jonsson H. A dimer method for finding saddle points on high dimensional potential surfaces using only first derivatives. *J Chem Phys* 1999, 111:7010–7022.
138. Kaestner J, Sherwood P. Superlinearly converging dimer method for transition state search. *J Chem Phys* 2008, 128:014106.
139. Shang C, Liu ZP. Constrained Broyden minimization combined with the dimer method for locating

 © 2011 John Wiley & Sons, Ltd.

17590884, 2011, 5, Downloaded from https://wires.onlinelibrary.wiley.com/doi/10.1002/wcms.34 by Research Institute for Healthcare Organization and Medical Management of Moscow Healthcare Department, Wiley Online Library on [12/05/2023]. See the Terms and Conditions (https://onlinelibrary.wiley.com/terms-and-conditions) on Wiley Online Library for rules of use; OA articles are governed by the applicable Creative Commons License

transition state of complex reactions. *J Chem Theory Comput* 2010, 6:1136–1144.

140. Heyden A, Bell AT, Keil FJ. Efficient methods for finding transition states in chemical reactions: comparison of improved dimer method and partitioned rational function optimization method. *J Chem Phys* 2005, 123:224101.
141. Pancir J. Calculation of the least energy path on the energy hypersurface. *Collect Czech Chem Commun* 1975, 40:1112–1118.
142. Basilevsky MV, Shamov AG. The local definition of the optimum ascent path on a multidimensional potential energy surface and its practical application for the location of saddle points. *Chem Phys* 1981, 60:347–358.
143. Hoffman DK, Nord RS, Ruedenberg K. Gradient extremals. *Theor Chim Acta* 1986, 69:265–279.
144. Jorgensen P, Jensen HJA, Helgaker T. A gradient extremal walking algorithm. *Theor Chim Acta* 1988, 73:55–65.
145. Schlegel HB. Following gradient extremal paths. *Theor Chim Acta* 1992, 83:15–20.
146. Sun JQ, Ruedenberg K. Gradient extremals and steepest descent lines on potential energy surfaces. *J Chem Phys* 1993, 98:9707–9714.
147. Bondensgård K, Jensen F. Gradient extremal bifurcation and turning points: an application to the H_2CO potential energy surface. *J Chem Phys* 1996, 104:8025–8031.
148. Smith CM. How to find a saddle point. *Int J Quantum Chem* 1990, 37:773–783.
149. Helgaker T. Transition state optimizations by trust-region image minimization. *Chem Phys Lett* 1991, 182:503–510.
150. Sun JQ, Ruedenberg K. Locating transition states by quadratic image gradient descent on potential energy surfaces. *J Chem Phys* 1994, 101:2157–2167.
151. McIver JW, Komornicki A. Structure of transition states in organic reactions. General theory and an application to the cyclobutene-butadiene isomerization using a semiempirical molecular orbital method. *J Am Chem Soc* 1972, 94:2625–2633.
152. Poppinger D. Calculation of transition states. *Chem Phys Lett* 1975, 35:550–554.
153. Komornicki A, Ishida K, Morokuma K, Ditchfield R, Conrad M. Efficient determination and characterization of transition states using *ab initio* methods. *Chem Phys Lett* 1977, 45:595–602.
154. Mueller K, Brown LD. Location of saddle points and minimum energy paths by a constrained simplex optimization procedure. *Theor Chim Acta* 1979, 53:75–93.
155. Dewar MJS, Healy EF, Stewart JJP. Location of transition states in reaction mechanisms. *J Chem Soc, Faraday Trans II* 1984, 80:227–233.
156. Ionova IV, Carter EA. Ridge method for finding saddle-points on potential energy surfaces. *J Chem Phys* 1993, 98:6377–6386.
157. Ionova IV, Carter EA. Direct inversion in the iterative subspace-induced acceleration of the ridge method for finding transition states. *J Chem Phys* 1995, 103:5437–5441.
158. Elber R, Karplus M. A method for determining reaction paths in large molecules: application to myoglobin. *Chem Phys Lett* 1987, 139:375–380.
159. Quapp W. Chemical reaction paths and calculus of variations. *Theor Chem Acc* 2008, 121:227–237.
160. Choi C, Elber R. Reaction path study of helix formation in tetrapeptides: effect of side chains. *J Chem Phys* 1991, 94:751–760.
161. Jónsson H, Mills G, Jacobsen W. Nudged elastic band method for finding minimum energy paths of transitions. In: Berne BJ, Cicotti G, Coker DF, eds. *Classical and Quantum Dynamics in Condensed Phase Simulations*. Singapore: World Scientific; 1998, 385.
162. Henkelman G, Jonsson H. Improved tangent estimate in the nudged elastic band method for finding minimum energy paths and saddle points. *J Chem Phys* 2000, 113:9978–9985.
163. Henkelman G, Uberuaga BP, Jonsson H. A climbing image nudged elastic band method for finding saddle points and minimum energy paths. *J Chem Phys* 2000, 113:9901–9904.
164. Trygubenko SA, Wales DJ. A doubly nudged elastic band method for finding transition states. *J Chem Phys* 2004, 120:2082–2094.
165. Chu JW, Trout BL, Brooks BR. A super-linear minimization scheme for the nudged elastic band method. *J Chem Phys* 2003, 119:12708–12717.
166. Maragakis P, Andreev SA, Brumer Y, Reichman DR, Kaxiras E. Adaptive nudged elastic band approach for transition state calculation. *J Chem Phys* 2002, 117:4651–4658.
167. Galvan IF, Field MJ. Improving the efficiency of the NEB reaction path finding algorithm. *J Comput Chem* 2008, 29:139–143.
168. Sheppard D, Terrell R, Henkelman G. Optimization methods for finding minimum energy paths. *J Chem Phys* 2008, 128:134106.
169. Alfonso DR, Jordan KD. A flexible nudged elastic band program for optimization of minimum energy pathways using *ab initio* electronic structure methods. *J Comput Chem* 2003, 24:990–996.
170. Gonzalez-Garcia N, Pu JZ, Gonzalez-Lafont A, Lluch JM, Truhlar DG. Searching for saddle points by using the nudged elastic band method: an implementation for gas-phase systems. *J Chem Theory Comput* 2006, 2:895–904.
171. E W, Ren WQ, Vanden-Eijnden E. String method for the study of rare events. *Phys Rev B* 2002, 66:052301.

17590884, 2011, 5, Downloaded from https://wires.onlinelibrary.wiley.com/doi/10.1002/wcms.34 by Research Institute for Healthcare Organization and Medical Management of Moscow Healthcare Department, Wiley Online Library on [12/05/2023]. See the Terms and Conditions (https://onlinelibrary.wiley.com/terms-and-conditions) on Wiley Online Library for rules of use; OA articles are governed by the applicable Creative Commons License

172. E W, Ren WQ, Vanden-Eijnden E. Simplified and improved string method for computing the minimum energy paths in barrier-crossing events. *J Chem Phys* 2007, 126:164103.
173. Ayala PY, Schlegel HB. A combined method for determining reaction paths, minima, and transition state geometries. *J Chem Phys* 1997, 107:375–384.
174. Burger SK, Yang WT. Quadratic string method for determining the minimum-energy path based on multiobjective optimization. *J Chem Phys* 2006, 124:054109.
175. Burger SK, Yang W. Sequential quadratic programming method for determining the minimum energy path. *J Chem Phys* 2007, 127:164107.
176. Koslover EF, Wales DJ. Comparison of double-ended transition state search methods. *J Chem Phys* 2007, 127:134102.
177. Truhlar DG, Garrett BC. Variational transition state theory. *Annu Rev Phys Chem* 1984, 35:159–189.
178. Miller WH, Handy NC, Adams JE. Reaction path Hamiltonian for polyatomic molecules. *J Chem Phys* 1980, 72:99–112.
179. Fukui K. The path of chemical reactions—the IRC approach. *Acc Chem Res* 1981, 14:363–368.
180. McKee ML, Page M. Computing reaction pathways on molecular potential energy surfaces. In: Lipkowitz KB, Boyd DB, eds. *Reviews in Computational Chemistry*. Vol 4. New York: VCH; 1993, 35–65.
181. Garrett BC, Redmon MJ, Steckler R, Truhlar DG, Baldridge KK, Bartol D, Schidt MW, Gordon MS. Algorithms and accuracy requirements for computing reaction paths by the method of steepest descent. *J Phys Chem* 1988, 92:1476–1488.
182. Gear CW. *Numerical Initial Value Problems in Ordinary Differential Equations*. Englewood Cliffs, NJ: Prentice-Hall; 1971.
183. Ishida K, Morokuma K, Komornicki A. The intrinsic reaction coordinate. An *ab initio* calculation for HNC $\rightarrow$ HCN and $H^- + CH_4 \rightarrow CH_4 + H^-$. *J Chem Phys* 1977, 66:2153–2156.
184. Page M, Doubleday C, McIver JW. Following steepest descent reaction paths. The use of higher energy derivatives with *ab initio* electronic structure methods. *J Chem Phys* 1990, 93:5634–5642.
185. Page M, McIver JM. On evaluating the reaction path Hamiltonian. *J Chem Phys* 1988, 88:922–935.
186. Sun JQ, Ruedenberg K. Quadratic steepest descent on potential energy surfaces. 1. Basic formalism and quantitative assessment. *J Chem Phys* 1993, 99:5257–5268.
187. Sun JQ, Ruedenberg K. Quadratic steepest descent on potential energy surfaces. 2. Reaction path following without analytical Hessians. *J Chem Phys* 1993, 99:5269–5275.
188. Eckert F, Werner HJ. Reaction path following by quadratic steepest descent. *Theor Chem Acc* 1998, 100:21–30.
189. Gonzalez C, Schlegel HB. An improved algorithm for reaction path following. *J Chem Phys* 1989, 90:2154–2161.
190. Gonzalez C, Schlegel HB. Reaction path following in mass-weighted internal coordinates. *J Phys Chem* 1990, 94:5523–5527.
191. Burger SK, Yang WT. Automatic integration of the reaction path using diagonally implicit Runge-Kutta methods. *J Chem Phys* 2006, 125:244108.
192. Burger SK, Yang WT. A combined explicit-implicit method for high accuracy reaction path integration. *J Chem Phys* 2006, 124:224102.
193. Stewart JJP, Davis LP, Burggraf LW. Semiempirical calculations of molecular trajectories: method and applications to some simple molecular systems. *J Comput Chem* 1987, 8:1117–1123.
194. Hratchian HP, Schlegel HB. Following reaction pathways using a damped classical trajectory algorithm. *J Phys Chem A* 2002, 106:165–169.
195. Hratchian HP, Schlegel HB. Accurate reaction paths using a Hessian based predictor-corrector integrator. *J Chem Phys* 2004, 120:9918–9924.
196. Hratchian HP, Schlegel HB. Using Hessian updating to increase the efficiency of a Hessian based predictor-corrector reaction path following method. *J Chem Theory Comput* 2005, 1:61–69.
197. Malick DK, Petersson GA, Montgomery JA. Transition states for chemical reactions. I. Geometry and classical barrier height. *J Chem Phys* 1998, 108:5704–5713.
198. Olender R, Elber R. Yet another look at the steepest descent path. *THEOCHEM* 1997, 398:63–71.
199. Vanden-Eijnden E, Heymann M. The geometric minimum action method for computing minimum energy paths. *J Chem Phys* 2008, 128:061103.
200. Aguilar-Mogas A, Crehuet R, Gimenez X, Bofill JM. Applications of analytic and geometry concepts of the theory of Calculus of Variations to the Intrinsic Reaction Coordinate model. *Mol Phys* 2007, 105:2475–2492.
201. Aguilar-Mogas A, Gimenez X, Bofill JM. Finding reaction paths using the potential energy as reaction coordinate. *J Chem Phys* 2008, 128:104102.

 © 2011 John Wiley & Sons, Ltd.

17590884, 2011, 5, Downloaded from https://wires.onlinelibrary.wiley.com/doi/10.1002/wcms.34 by Research Institute for Healthcare Organization and Medical Management of Moscow Healthcare Department, Wiley Online Library on [12/05/2023]. See the Terms and Conditions (https://onlinelibrary.wiley.com/terms-and-conditions) on Wiley Online Library for rules of use; OA articles are governed by the applicable Creative Commons License